

國立台灣大學醫學院分子醫學研究所



碩士論文

Institute of Molecular Medicine

College of Medicine

National Taiwan University

Master Thesis

E3 泛素連接酶 ZNRF1 調控 TLR7 及 TLR9

訊息傳遞之研究

Study on the Regulation of E3 Ubiquitin Ligase ZNRF1
in the TLR7- and TLR9-mediated Signaling Pathways

盧麒安

Chi-An Lu

指導教授：徐立中 博士

Advisor: Li-Chung Hsu, Ph.D.

中華民國 109 年 7 月

July 2020

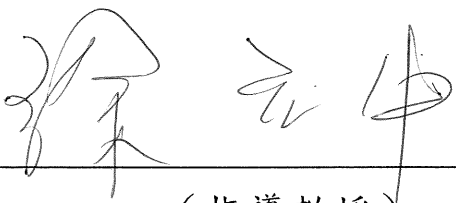
國立臺灣大學碩士學位論文 口試委員會審定書

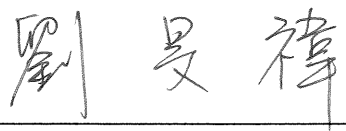
E3 泛素連接酶 ZNRF1 調控 TLR7 及 TLR9 訊息傳遞之研究

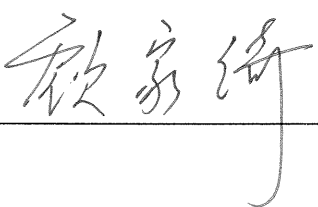
Study on the Regulation of E3 Ubiquitin Ligase ZNRF1 in
the TLR7- and TLR9-mediated Signaling Pathways

本論文係盧麒安君（R07448002）在國立臺灣大學分子醫學研究所完成之碩士學位論文，於民國 109 年 7 月 28 日承下列考試委員審查通過及口試及格，特此證明

口試委員：

 (簽名)
(指導教授)





系主任、所長

 (簽名)



致謝

兩年前，我站在人生的十字路口迷茫，究竟要踏上中等教育之路，抑或是就讀研究所精進自己在生命科學領域的能力。在修習教育學程的時候，我就不斷尋找著科學教育的答案，與其似懂非懂地記下複雜的教育理論及流程，不如到分醫所親身體驗一回做研究的生活。紮實的課程以及實驗訓練，讓我不論是在英文能力還是邏輯思考上都獲益良多。

首先，我要感謝我的指導老師徐立中老師，對於理解力不好的我，老師總是很耐心地畫圖教我，提供許多實驗上的建議以及觀念上的修正，最後這段日子更是感謝老師很用心地修改我的論文，讓我可以學到更精準的英文寫作用法。此外，也很謝謝老師時常關心我的身體，甚至在我最虛弱的时候幫我找到適合我的醫師。再來要感謝我的口委顧家綺老師及劉旻禕老師，在進度報告和口試時提供許多很好的建議及方向，猶如醍醐灌頂般讓我能用更不同的角度切入我的研究。另外要感謝免疫所李建國老師及其實驗室的成員又綾學姐提供血清，感謝微生物所張永祺老師提供病毒，感謝劉旻禕老師及其實驗室成員幸芙學姐提供配體及抗體。感謝林國儀老師及其實驗室成員怡安學姐提供細胞及實驗上的建議。感謝李芳仁老師實驗室的婉筠學姐和佩娟同學教我酵母菌的實驗。感謝分醫所老師們認真指導課業，感謝潘俊良老師對我說雄中生要加油，感謝分醫所助教們辛苦地處理行政事務。感謝實驗動物中心的鍾小姐，幫我協調各類的問題。


我能走到這裡，真的是要好好感謝實驗室的大家。首先是教我非常多實驗技術和邏輯思考的祐聖學長，是他讓我找到科學教育的答案，除了幫我打好基礎，也在我遇到問題的時候出手相救，他真的是一個很厲害的科學家。感謝聖揚學姐和佳靜學姐，不厭其煩地在實驗上給予很多協助，也帶給我很多歡樂。感謝晏如、蕙萱、湘怡、懿姍學姐和鼎翔學長教過我實驗並且一直給予精神上的支持。感謝我的好同學亭妤，跟我一起克服挑戰完成學業。感謝翊庭和靖之學妹平時的加油打氣，感謝立倫、懷瑜學弟和季昀學妹陪我吃飯並且給我很多鼓勵，沒有我還是要記得吃飯。感謝實驗室其他學長姐及學弟妹，在很多事情上提供幫忙與建議。非常謝謝大家的幫助，這份感動我會銘記在心。

碩班生涯遇到挫折的時候，也感謝從小到大認識的朋友們，除了在精神上給予支持與鼓勵，也在一些問題上互相幫忙。另外要感謝我的表妹，在畫圖上給予協助。最後要感謝我的家人，提供經濟援助以及心靈上的扶持。要感謝的人實在太多，難以用規定格式限定的一頁表達我最真誠的感謝，真的很謝謝大家，讓我能夠在這兩年的時間裡滿載而歸，繼續朝著教育之路邁進，希望有朝一日各位有需要我協助的時候也可以想到我，我會盡我所能地幫忙。

摘要



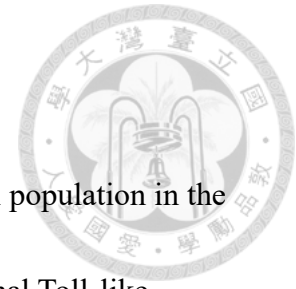
漿狀樹突細胞 (plasmacytoid dendritic cells) 是哺乳類先天免疫系統中一群扮演哨兵角色的細胞，它們高度表現第七型及第九型類鐸受體 (Toll-like receptor 7 and 9)，此二類鐸受體能分別偵測單股核糖核酸 (single-strand RNA) 及未甲基化的 CpG 位點去氧核糖核酸 (CpG DNA)。當第七型及第九型類鐸受體偵測到配體後，漿狀樹突細胞會立即產生大量的第一型干擾素 (type I interferons) 來抑制病毒的複製並且促進周圍細胞的抗病毒功能。ZNR1 (Zinc and ring finger 1) 是一種 E3 泛素連接酶，過去被報導在瓦氏退化現象 (Wallerian degeneration) 中扮演重要角色。我們實驗室先前的研究發現 ZNR1 在第四型類鐸受體 (Toll-like receptor 4) 的活化下會增加促發炎細胞激素 (pro-inflammatory cytokine) 並減少抗發炎細胞激素中的白血球介白素-10 (interleukin 10)，顯示 ZNR1 在第四型類鐸受體所誘導的發炎反應中扮演正向調節的角色。我們也進一步發現，當類 FMS 的酪氨酸激酶-3 受體所分化的漿狀樹突細胞 (Flt3L-driven pDCs) 及人類的漿狀樹突細胞株 (CAL-1) 中的第七型及第九型類鐸受體活化後，ZNR1 缺失會增強第一型干擾素產生。在這篇研究中，我們試圖去探討在第七型及第九型類鐸受體所誘導的免疫反應中，ZNR1 的詳細調控機制以及在此過程中 ZNR1 是如何被活化。我們首先確認用第七型及第九型類鐸配體刺激人類的漿狀樹突細胞株 (CAL-1) 後，ZNR1 缺失會增強第一型干擾素產生。在 ZNR1 缺失的人類漿狀樹突細胞株 (CAL-1) 中，第七型類鐸受體的活化會增加 IKK α 、MAPK 及 IKK β /NF- κ B 的活化，而第九型類



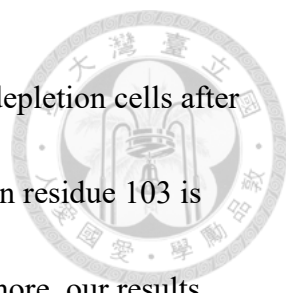
鐸受體的活化僅會增加的活化。此外，在 ZNRF1 103 號的酪氨酸對於第七型及第九型類鐸受體所誘導的免疫反應是重要的。我們的動物實驗結果顯示在流感病毒 H5N1 的感染下 IKK α ，ZNRF1 缺失的小鼠相較於野生型小鼠表現更高的存活率。在流感病毒 H5N1 感染後第六天，ZNRF1 缺失小鼠肺臟中的促發炎細胞激素、第一型干擾素、趨化介素及病毒的 mRNA 都有較低的情形。然而，究竟 ZNRF1 缺失在小鼠身上會影響病毒的清除還是細胞激素的產生仍有待之後的實驗釐清。總結以上，我們的結果顯示在漿狀樹突細胞中，ZNRF1 可能會透過控制類鐸受體的運輸而負向調節第七型及第九型類鐸受體所驅動的免疫反應。

關鍵字：第一型鋅暨環指泛素連接酶、漿狀樹突細胞、第七型類鐸受體、第九型類鐸受體、第一型干擾素、流感病毒

Abstract



Plasmacytoid dendritic cells (pDCs), a unique sentinel cell population in the mammalian innate immunity system, express high levels of endosomal Toll-like receptors (TLRs) TLR7 and TLR9, which sense single-strand RNA (ssRNA) and unmethylated CpG DNA, respectively. Upon engagement of TLR7 and TLR9, pDCs produce massive quantities of type I interferons (IFNs) rapidly to inhibit viral replication and promote the antiviral functions in surrounding cells. Zinc and ring finger 1 (ZNR1) is an E3 ubiquitin ligase, which plays a crucial role in Wallerian degeneration. Previous study in our lab demonstrated that ZNR1 enhanced the production of pro-inflammatory cytokines and reduced anti-inflammatory cytokine IL-10 upon TLR4 activation, suggesting its positive regulatory role in TLR4-triggered inflammatory response. We further demonstrated that ZNR1 depletion enhanced type I interferons in both FMS-like tyrosine kinase 3 ligand (Flt3L)-driven pDCs and CAL-1 cells (human pDCs) upon TLR7 and TLR9 activation. In this study, we aim to reveal the detailed mechanism by which ZNR1 regulates TLR7- and TLR9-mediated immune responses and how ZNR1 is activated upon engagement of TLR7 and TLR9. We confirmed that ZNR1 depletion enhanced type I interferon production in CAL-1 cells after stimulation of TLR7 and TLR9 ligands. Activation of IKK α , MAPKs and IKK β /NF- κ B was increased in ZNR1-depleted CAL-1 cells after TLR7 engagement.



However, only increased IKK α activation was observed in ZNRF1 depletion cells after TLR9 activation. In addition, tyrosine phosphorylation site ZNRF1 on residue 103 is required for TLR7- and TLR9-mediated immune responses. Furthermore, our results showed that ZNRF1 knockout mice displayed better survival compared with wildtype mice after challenged with H5N1 influenza virus (IAV). Lower levels of pro-inflammatory cytokine, type I interferons, chemokines and viral mRNA were decreased in *Znrf1*^{-/-} lungs at day 6 after intratrachea infection of H5N1 IAV. Nevertheless, it remains to be further investigated whether depletion of ZNRF1 in mice affects viral clearance or cytokine production. Taken together, our results suggest that ZNRF1 is a negative regulator of TLR7- and TLR9-driven immune response in pDCs possible through controlling receptor trafficking.

Keywords: Zinc and ring finger 1, plasmacytoid dendritic cell, Toll-like receptor 7, Toll-like receptor 9, type I interferon, influenza virus

Contents



致謝	i
摘要	ii
Abstract.....	iv
Contents.....	vi
Introduction	1
Inflammation	1
Pattern-recognition receptors (PRRs).....	1
Toll-like receptors (TLRs).....	3
TLRs signaling pathway.....	4
Nucleic acid-sensing TLRs.....	5
TLR7/9 in antiviral immunity	6
TLR7/9 signaling pathway in pDCs	6
Type I interferon signaling.....	8
TLR7/9 trafficking.....	8
Proteolytic cleavage of TLR7/9.....	11
Ubiquitination.....	12
Ubiquitination in TLR-mediated immune responses.....	13
Zinc and RING finger 1 (ZNR1).....	14
ZNR1 and immunity.....	16
Aim	17
Material and Methods	18
Reagents and antibodies	18
Mice.....	19
Preparation of Flt3L-induced bone marrow-derived pDCs (Flt3L-pDCs).....	20
Preparation of Flt3L-pDCs	21
Cell culture	22
Generation of ZNR1 knockout CAL-1 cells using CRISPR/Cas9 system.....	22
Genomic DNA extraction and sequence alignment.....	23
RNA extraction and quantitative RT-PCR (RT-qPCR).....	24
Cell lysates preparation	28
Immunoblotting	29
Ligand internalization assay	30
Immunoprecipitation	30
Ubiquitination assay	31
Cytosolic and nuclear extract fractionation	31

Virus amplification	32
Intratracheal instillation.....	33
Infiltrating cells isolation.....	34
Statistical analysis	35
Results	36
ZNR1 depletion in Flt3L-pDCs enhances the production of type I IFNs and pro-inflammatory cytokines upon TLR7 and TLR9 activation.....	36
ZNR1 depletion promotes increased amount of type I IFNs in CAL-1 upon TLR7 activation.....	36
ZNR1 depletion enhances IKK α activation and nuclear translocation of IRF7 upon TLR7 activation in CAL-1 cells.	37
ZNR1 depletion promotes TLR7-induced MAPK and IKK β /NF- κ B activation in CAL-1 cells.	40
ZNR1 Y103 residue is important for its regulatory function in TLR7 signaling. 40	
ZNR1 depletion promotes increased amount of type I IFNs in CAL-1 upon TLR9 activation.	41
ZNR1 depletion enhances IKK α activation and nuclear translocation of IRF7 but has little impact on MAPK activation upon TLR9 activation in CAL-1 cells.	42
ZNR1 Y103 residue is important for its regulatory function in TLR9 signaling. 43	
ZNR1 deficient mice are resistant to H5N1 influenza A virus infection.	43
Discussion.....	45
The possible role of ZNR1 in TLR7 and TLR9 trafficking	45
The possible role of ZNR1 in ubiquitination of TLR7/9.....	47
The possible role of phosphorylation at Y103 of ZNR1 in TLR7- and TLR9-induced signaling pathway	48
The possible role of ZNR1 during H5N1 influenza virus infection.....	49
Figures	51
Figure 1. ZNR1 depletion enhances TLR7-triggered type I IFNs and pro-inflammatory cytokines in Flt3L-pDCs.....	51
Figure 2. ZNR1 depletion enhances TLR9-triggered type I IFNs and pro-inflammatory cytokines in Flt3L-pDCs.....	52
Figure 3. Generation of <i>ZNR1</i> ^{-/-} CAL-1 cells by CRISPR/Cas9 system.....	53
Figure 4. Depletion of ZNR1 enhances TLR7-induced type I IFNs and pro-inflammatory cytokines in CAL-1 cells	54
Figure 5. ZNR1 deficiency enhances IKK α activation in CAL-1 cells after stimulation with R848	55
Figure 6. ZNR1 deficiency increases IRF7 activation in CAL-1 cells after stimulation with R848	56

Figure 7. ZNRF1 deficiency in CAL-1 cells enhances STAT1 activation and the expression of interferon-stimulated genes <i>CXCL10</i> and <i>OAS1</i> after stimulation with R848	57
Figure 8. ZNRF1 is not involved in the type I IFN signaling pathway.	59
Figure 9. ZNRF1 deficiency enhances MAPK activation in CAL-1 cells after stimulation with R848	61
Figure 10. ZNRF1 Y103 is critical for TLR7-induced IKK α , MAPKs and IKK β /NF- κ B activation.....	63
Figure 11. ZNRF1 depletion induced TLR9-driven type I IFNs but not pro-inflammatory cytokines production in CAL-1 cells.....	64
Figure 12. ZNRF1 deficiency promotes IKK α activation in CAL-1 cells after TLR9 activation.....	65
Figure 13. ZNRF1 deficiency enhances IRF7 activation in CAL-1 cells after stimulation with CpGA.....	66
Figure 14. ZNRF1 deficiency in CAL-1 cells enhances STAT1 activation and the expression of interferon-stimulated genes <i>CXCL10</i> and <i>OAS1</i> upon TLR9 activation	67
Figure 15. ZNRF1 deficiency in CAL-1 cells has little impact on MAPK activation after stimulation with CpGA	69
Figure 16. Y103 of ZNRF1 is critical for TLR9-induced IKK α and AKT activation	71
Figure 17. <i>Znrf1</i> ^{-/-} mice are more resistant to H5N1 influenza virus infection.	72
Figure 18. <i>Znrf1</i> ^{-/-} mice displayed reduced levels of pro-inflammatory cytokines and chemokines after H5N1 influenza virus infection	75
Figure 19. <i>Znrf1</i> ^{-/-} mice showed reduced numbers of alveolar macrophages, conventional DCs and neutrophils in lungs after influenza virus H5N1 infection.	77
Figure 20. The proposed model for the regulation of TLR7 and TLR9-mediated immune response by ZNRF1 in pDCs.....	78
References	80

Introduction

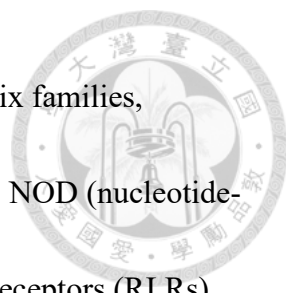


Inflammation

Inflammation is a protective process in our body to remove harmful invaders and repair damaged tissues. It can be triggered by environmental agents, toxic chemicals, trauma and microbial infection. Inflammation is classically characterized by five symptoms: erythema, heat, edema, pain and loss of tissue function. During inflammation, increased permeability of the vascular endothelium allows immune cells to extravasate into the sites of infection or tissue damage, leading to elimination of pathogens and infected or dead cells [1].

Pattern-recognition receptors (PRRs)

The innate immune system is the first line of host defense against pathogenic infection. It can cause inflammatory responses upon microbial infection or tissue damage [2,3]. There are specialized germline encoded receptors called pattern recognition receptors (PRRs), which can recognize pathogen-associated molecular patterns (PAMPs), the conserved structures existing among microbes. They also can recognize damage-associated molecular patterns (DAMPs) which are endogenous molecules released from damaged tissues or dead cells [4].



Based on protein domain analysis, PRRs can be classified into six families, including Toll-like receptors (TLRs), C-type lectin receptors (CLRs), NOD (nucleotide-binding oligomerization domain)-like receptors (NLRs), RIG-I-like receptors (RLRs), AIM2-like receptors (ALRs) and the intracellular DNA sensors including Cyclic GMP-AMP synthase (cGAS) [5,6]. These families can be separated into two subclasses according to their cellular localization. TLRs and CLRs families are membrane-bound receptors localized at the cell surface or endocytic compartments, where they detect PAMPs and DAMPs in the extracellular space or the endosomal lumen. RLRs, ALRs and, NLRs families, and cGAS are located in the cytoplasm, where they sense their ligands derived from intracellular pathogens.

Except for some NLRs, detection of PAMPs or DAMPs by PRRs activates a series of intracellular signaling events leading to upregulation of genes involved in inflammatory responses, including type I interferons (IFNs), pro-inflammatory cytokines, chemokines, antimicrobial proteins, cell adhesion molecules and immunoreceptors [2,7]. They together take part in the early phase of host defense against pathogenic infection and initiate sequent adaptive immune responses.


Regulation of PRR driven immune responses can be at the transcriptional, post-transcriptional, translational, or post-translational levels. Transcriptional regulatory mechanism mainly focuses on the activation of different transcription factors that

induce the production of type I interferons (IFNs) and pro-inflammatory cytokines.

Type I interferons play a crucial role in antiviral immunity [8]. The pro-inflammatory cytokines such as tumor necrosis factor (TNF), interleukin (IL)-1, and IL-6 regulate hematopoiesis, the permeability of blood vessels, and the recruitment of immune cells to the inflammatory sites [2]. On the other hand, post-transcriptional regulation can control alternative splicing and polyadenylation of pre-mRNA and mRNA stability, protein translation and post-translational modification (PTM) [9]. In addition, PRRs activation regulates cell death, phagocytosis and autophagy [10]. Tight regulation of these control mechanisms allows the host to defend against invading pathogens without causing too harmful tissue damage. However, abnormal activation of PRRs signaling is associated with the pathogenesis of many diseases, including inflammatory disorders and autoimmune diseases [11].

Toll-like receptors (TLRs)


Among PRRs, Toll-like receptors (TLRs) family is first identified and the best characterized. In 1985, Christiane Nüsslein-Volhard first discovered Toll, which regulates dorsal-ventral polarity pattern of the *Drosophila* embryo [12]. In 1996, Jules A Hoffmann found that Toll controls the antifungal response in *Drosophila*, first uncovering the important function of TLRs in the immune system [13]. The TLR family



consists of 10 members (TLR1-TLR10) in human and 12 (TLR1-TLR9, TLR11-13) in mouse [14]. According to their subcellular localization, TLRs can be classified into two subfamilies. TLR1, TLR2, TLR4, TLR5, TLR6, and TLR10 locate on the cell surface, whose ligands include lipoproteins, peptidoglycans, zymosan, lipopolysaccharide (LPS), and flagellin existing on the surface of pathogens. On the other hand, TLR3, TLR7, TLR8, TLR9, TLR11, TLR12, and TLR13 are localized in the endosomes, where they recognize their ligands, nucleic acids, from pathogens or dead cells [15,16]. TLRs are expressed not only in immune cells, including macrophages and dendritic cells, but also in nonimmune cells such as fibroblast and epithelial cells. TLR comprises an ectodomain containing leucine-rich repeats (LRRs) which mediate PAMPs recognition, a transmembrane domain, and a cytoplasmic tail containing the Toll/IL-1R homology (TIR) domain that initiates downstream signal transduction upon ligand engagement [14].

TLRs signaling pathway

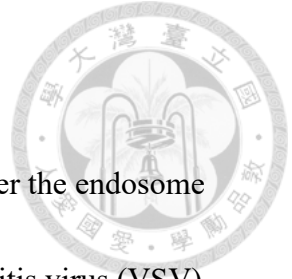
Upon recognition of PAMPs or DAMPs, TLR receptors form homo- or hetero-dimer and then recruits TIR-domain-containing adaptor proteins either myeloid differentiation primary response protein 88 (MyD88) and/or MyD88-adaptor-like protein (MAL) or TIR-domain-containing adaptor protein inducing IFN β (TRIF) and/or



TRIF-related adaptor molecule (TRAM) via homotypic TIR-TIR domain interactions [15,17]. The TLRs-MyD88 or TLRs-TRIF complex then induce a series of signaling cascades leading to activation of IKK/nuclear-factor- κ B (NF- κ B), mitogen-activated protein kinases (MAPKs) and interferon-regulatory factors (IRFs), all of which are required for induction of inflammatory cytokines and type I interferons. Both inflammatory cytokines and type I interferons contribute to host defense against invading pathogens [14].

Nucleic acid-sensing TLRs

The ligands of endosomal TLRs are nucleic acid. For example, TLR3 recognizes double-stranded RNA (dsRNA); TLR7/8 respond to single-stranded RNA (ssRNA); TLR9 detects unmethylated or hypomethylated CpG-containing DNA; TLR13 recognizes bacterial ribosomal RNA [18-21]. These endosomal TLRs, thereby, are called nucleic acid-sensing TLRs. Recognition of foreign nucleic acid is crucial for efficient immunity against pathogens, whereas recognition of self-nucleic acids by endosomal TLRs leads to the pathologies associated with autoimmune or autoinflammatory diseases. Thus, precise regulation of endosomal TLRs activation via different mechanisms, including receptor proteolytic cleavage and trafficking, is important to constrain the immune responses triggered by self-nucleic acids [18].




TLR7/9 in antiviral immunity

It has been shown that TLR7 recognizes ssRNA viruses that enter the endosome via endocytosis [22], including influenza virus [23], vesicular stomatitis virus (VSV) [24], human immunodeficiency virus-1 (HIV-1) [25], paramyxovirus [26], hepatitis C virus (HCV) [27] and coronavirus [28]. TLR9 recognizes DNA viruses such as mouse cytomegalovirus (MCMV) [29], herpes simplex virus-1 (HSV-1) [30], herpes simplex virus-2 (HSV-2) [31] and poxvirus [32].

TLR7 and TLR9 are highly expressed in plasmacytoid dendritic cells (pDCs) which are unique sentinel cells defending against viruses at the forefront [33]. Upon recognition of ssRNA or dsDNA, pDCs secrete massive type I interferons through TLR7/9 and downstream IRF7 [34]. Type I IFNs further trigger host antiviral response, recruit, and activate various immune cells such as NK cells, monocytes, myeloid dendritic cells (mDCs), B cells, and T cells. In addition, pDCs produce pro-inflammatory cytokines, chemokines and type III interferons such as IFN λ and IL-28/29, all of which contribute to both innate and adaptive immune responses [33]. Thus, pDCs provide a link between the innate and adaptive immune systems [35].

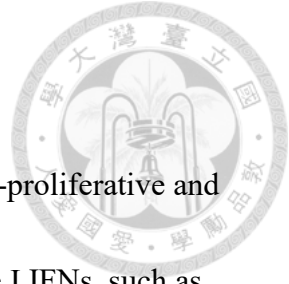
TLR7/9 signaling pathway in pDCs

Upon engagement, TLR7 or TLR9 associates with the adaptor protein MyD88,



which then recruits interleukin-1 receptor (IL-1R)-associated kinase (IRAK) 4, IRAK1/2 to form a complex called Myddosome. The complex then associates with tumour-necrosis factor (TNF)-receptor-associated factor (TRAF3), I κ B kinase (IKK) α , Osteopontin (OPN), Dedicator of cytokinesis 2 (Dock-2) and phosphoinositide 3-kinase (PI3K) [2,14,17,36-38]. This complex then activates interferon-regulatory factor 7 (IRF7) through phosphorylation by IKK α and/or IRAK1, resulting IRF7 translocation into the nucleus to induce type I IFNs expression.

In addition, IRAK4 activates IRAK1, and phosphorylated IRAK1 further interacts with TRAF6. TRAF6 then activates TAK1/TAB (TGF- β -activated kinase) by promoting the ubiquitination and activation of TAK1/TAB complex. TAK1 subsequently induces phosphorylation and activation of I κ B α -Kinase (IKK) complex. Activated IKK β promotes the phosphorylation and degradation of I κ B α , thereby releasing transcription factor nuclear-factor- κ B (NF- κ B) to translocate into the nucleus. In addition, TAK1/TAB complex also triggers the activation of mitogen-activated protein kinases (MAPKs), such as JNK, p38 and ERK, causing the phosphorylation and nuclear translocation of cyclic AMP-responsive element-binding protein (CREB) and activator protein 1 (AP1). The activation of these transcriptional factors all leads to induce the expression of pro-inflammatory cytokines and chemokines.




Type I interferon signaling

Type I interferons (IFNs) are cytokines exhibiting antiviral, anti-proliferative and immunomodulatory properties [39-40]. There are many kinds of type I IFNs, such as IFN α , IFN β , IFN ϵ , IFN κ , IFN ω (human) and IFN zeta/limitin (mouse) [41]. All type I IFNs bind to IFN receptor (IFNAR) composed of IFNAR1 and IFNAR2 subunits. Upon ligand engagement, IFNAR1 and IFNAR2 associate with tyrosine kinase 2 (TYK2) and Janus activated kinase 1 (JAK1), respectively, resulting in tyrosine phosphorylation of signal transducer and activator of transcription (STAT) 1 and STAT2. IFN-regulatory factor 9 (IRF9) is then recruited to the STAT1/STAT2 complex and the whole complex translocates to the nucleus to induce the production of IFN stimulated genes (ISGs) for defending against virus.

TLR7/9 trafficking

TLR7 and TLR9 are synthesized at ER, and their protein folding process are regulated by folding chaperones gp96 and PRAT4A [18, 42-43]. The trafficking of endosomal TLRs, including TLR7 and TLR9, from endoplasmic reticulum (ER) to the endosomes is controlled by the chaperone protein Unc-93 homolog B1 (UNC93B1).


Previous studies were shown that a single point mutation in the transmembrane domains of UNC93B1 (H412R) that abolishes its interaction with endosomal TLRs fails to



deliver receptors to the endosomal compartment, thereby abolishing TLRs signaling [18, 44-45]. It was reported that TLR9 outcompetes TLR7 for UNC93B1-mediated trafficking due to its higher binding affinity to UNC93B1 [46]. In addition, the involvement of UNC93B1 in TLR7 and TLR9 signaling is different in the endosomes. TLR9 must disassociate from UNC93B1 upon reaching the endosomes in order to allow the receptor to bind its ligand efficiently and initiate downstream signaling [47]. In contrast, UNC93B1 continuously associates with TLR7 in the endosomes, which is required for the recruitment of syntenin-1 to the receptor and facilitates the sorting of TLR7-UNC93B1 complex into intraluminal vesicles (ILV) of multivesicular bodies (MVB), resulting in termination of signaling to avoid excess inflammation [48].

After exiting ER, another ER membrane protein leucine-rich repeat containing protein 59 (LRRC59) helps load TLR7/9 into the coat protein complex II (COPII) vesicles, that are further transported to the Golgi [50]. Recruitment of sorting complex adaptor protein 4 (AP-4) is essential for TLR7 trafficking from trans-Golgi network to the endosomes directly, whereas TLR9 translocates to the cell surface first and subsequently transfers to the endosomes through endocytosis mediated by the adaptor protein 2 (AP-2) [18, 49].

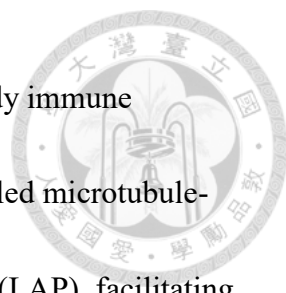
Accumulated data have shown that different types of endosomal compartments transmit distinct signaling to induce the expression of either type I interferons or pro-



inflammatory cytokines driven by NF- κ B [49, 52]. Interestingly, synthetic TLR9 ligands oligodinucleotides (ODNs) containing different sequences activate distinct signaling pathway in pDCs [53]. For instance, CpG-A ODN, which contains poly-G tails, preferentially forms large complexes and traffics to early endosome where TLR9 activates IRF7 signaling pathway, resulting in a robust type I interferons production. In contrast, monomeric CpG-B ODN, preferentially traffics to late endosome where TLR9 activates NF- κ B signaling pathway, leading to the production of pro-inflammatory cytokine. However, the single-stranded form of CpG-A generated by heating and flash cooling significantly reduces type I interferons expression. Conversely, when CpG-B is mixed with PMXB or conjugated with polysaccharide Ficoll, ODN dramatically enhances type I interferons production [53].

In addition, the adaptor protein-3 (AP-3) which locates at the endosomal membrane associates with IRF7, TRAF3 and matured TLR9. This complex is then sorted from the endosomes to the lysosome-related organelles (LROs) and further induces a robust type I interferons production [54]. Moreover, Hermansky-Pudlak syndrome (HPS) proteins BLOC-1 and BLOC-2 which are involved in biogenesis of LRO, as well as obscure solute channel protein Slc15a4 are crucial for TLR7 and TLR9 signaling in pDCs [55].

Besides early endosomes and LROs, another specialized compartment involves in



TLR9-mediated type I IFN response. Internalization of DNA-antibody immune complexes (DNA-IC) activates noncanonical autophagy pathway called microtubule-associated protein 1A/1B-light chain (LC3)-associated phagocytosis (LAP), facilitating TLR9 trafficking to this specialized interferon signaling compartment [56]. Notably, IFN- α production is not impaired in *Ap3b1*-deficient pDCs in response to DNA-IC, suggesting that this specialized compartment is totally different from AP-3-dependent LROs. Thus, different types of cargos transport to distinct compartments to trigger type I IFNs in pDCs.

Proteolytic cleavage of TLR7/9

Previous studies were demonstrated that TLR7/9 undergo proteolytic cleavage by asparagine endopeptidase and cathepsins, which allows cleaved receptor to recruit downstream molecules and induce signaling. This mechanism can prevent abnormal activation of TLR7/9 in response to self nucleic acids in the ER and Golgi apparatus [57, 58]. The cleavage process occurs in the endosomes where the decreased pH value is required for the enzymatic activity of asparagine endopeptidase (AEP) and multiple cathepsins [59]. The ectodomain of TLR7/9 is cleaved by these proteases and the N-terminal half of the ectodomain still associates with truncated receptors. Recent studies even showed that the N-terminal fragments of TLR7 and TLR9 are required for their

ligands binding initiation of downstream signaling in the endosomes. In the case of TLR7, the N-terminus is linked to the C-terminus by disulfide bonds [60, 61]. After proteolytic cleavage, truncated TLR7/9 can recruit the adaptor protein, MyD88, and activate the signaling pathway upon ligand binding.

Ubiquitination

Ubiquitination is a dynamic posttranslational modification (PTM) that involves covalent conjugation of 76-amino acid protein ubiquitin to the lysine residues of target proteins [62-63]. The process of ubiquitination includes three enzymatic steps which utilizes E1 ubiquitin-activating, E2 ubiquitin-conjugating and E3 ubiquitin-ligating enzymes. Ubiquitin can be further modified by ubiquitin-like molecules, such as SUMO, acetylation, or phosphorylation, creating distinct signals which lead to different cellular outcomes. Notably, ubiquitin contains seven lysine residues, and each of which can be ubiquitinated to build isopeptide-linked ubiquitin chains. In addition, ubiquitin molecules can be attached via the head-to-tail linkage called Met1-linked or linear ubiquitination. Moreover, these conjugated ubiquitin chains can be cleaved by ubiquitin-specific proteases called deubiquitinases (DUBs) [64].

These eight different polyubiquitin linkages lead to different cellular consequences, known as the ‘ubiquitin code’. For instance, K48-linked polyubiquitin chains are the

most abundant linkage type in the cell and are used for targeting proteins for proteasome degradation referred to as the ‘molecular kiss of death’ [65]. In contrast, K63-linked polyubiquitin chains play a nondegradative role and are involved in protein trafficking [66], DNA damage repair [67], transcriptional regulation [68] and signal transduction [69].

Ubiquitination in TLR-mediated immune responses

Ubiquitination is crucial for regulation of TLR-mediated immune responses. Upon TLRs activation, MyD88, IRAK1, and IRAK4 are recruited to the receptors to form the Myddosome complex. IRAK4 phosphorylates IRAK1, which further activates the E3 ubiquitin ligase TRAF6. TRAF6 together with the E2 ubiquitin complex, which is composed of Ubc13 and Uev1A, catalyzes K63-linked polyubiquitin chains conjugated to itself and NEMO or unanchored K63-linked polyubiquitin chains that associates with TAB2 subunit of TAK1 kinase complex and promotes its autophosphorylation and activation. The K63-linked polyubiquitin chains on TRAF6 serve as a platform for the recruitment of TAK1 and IKK. TAK1 is known to induce the phosphorylation and activation of IKK β and MAPK. I κ B α is then phosphorylated by activated IKK and subsequently polyubiquitinated by the Skp1-Cul1-F-box ubiquitin ligase (SCF- β TrCP) complex and degraded by the 26S proteasome. The transcription factor NF- κ B is then

released and translocated to the nucleus and induce the expression of target genes [70].

In TLR7/9-driven signaling, the ubiquitin ligase activity of TRAF6 is required for IRF7 and NF- κ B activation in pDCs [71, 72]. Upon activation, TLR9, and supposedly TLR7, is ubiquitinated by a yet-to-be-identified E3 ubiquitin ligase in pDCs. The ubiquitinated receptor is recognized by the hepatocyte growth factor-regulated tyrosine kinase substrate (HRS), facilitating the sorting of TLR9 to the multivesicular bodies (MVBs) through noncanonical endosomal sorting complexes required for transport (ESCRT) pathway, which eventually leads to termination of TLR9 signaling. [73].

Zinc and RING finger 1 (ZNRF1)

In 2001, T. Araki first identified a novel gene *nin283* (was renamed *Znrf1* later), which is induced in Schwann cells upon nerve injury [74]. ZNRF1 is a 227-amino acids protein that contains a zinc finger and a RING finger. It is expressed in the central nervous system and peripheral ganglia. ZNRF1 is predicted to be mainly located in the endosomes and lysosomes.

Many proteins containing the RING finger have been suggested to possess an E3 ubiquitin ligase activity because this motif can recruit specific E2s [75]. Indeed, *in vitro* ubiquitination assays showed that ZNRF1 exhibited an E3 ubiquitin ligase activity together with Ubc4 and UbcH5C, indicating that ZNRF1 functions as an E3 ubiquitin

ligase [76]. A point mutation at cysteine 184 of ZNRF1, which disrupts its RING finger structure abolishes the E3 ligase activity of ZNRF1, whereas mutation of cysteine 145 which disrupts its zinc finger structure, had little effect on the E3 ligase activity. Taken together, only the RING finger motif is required for the E3 ligase activity of ZNRF1.

The residues 1-10 of ZNRF1 N-terminal region contain the N-myristoylation signals which can target ZNRF1 to cellular compartments. Additional residues within the N-terminal domain of ZNRF1 are also necessary for its appropriate localization at the endosomes and the lysosomes [76]. In addition, ZNRF1 was reported to play a role in regulating the Ca^{2+} -dependent exocytosis.

ZNRF1 was previously reported to function as a crucial regulator in neuron degeneration [77]. ZNRF1 was shown to target AKT for degradation through the ubiquitin-proteasome system. This further induced GSK3B-dependent CRMP2 phosphorylation and eventually promoted Wallerian degeneration. The same research group further revealed that oxidative stress activates ZNRF1 by inducing phosphorylation at tyrosine 103 residue of ZNRF1 mediated by epidermal growth factor receptor (EGFR), resulting in Wallerian degeneration and neuronal apoptosis [78]. The phosphorylation-resistant mutant ZNRF1-Y103F protects neurons from oxidative stress-induced apoptosis, which is similar to the phenotype caused by the enzyme-dead mutant ZNRF1-C184A. These data indicate that ZNRF1 plays roles in neurodegenerative

pathways.

ZNRF1 has been linked to human diseases. It was reported that ZNRF1 may be related to leukemogenesis of B cell acute lymphoblastic leukemia (B-ALL) with alternation of PAX5, a paired box domain (PBD) transcription factor required for B cell differentiation [79].

ZNRF1 and immunity

In contrast to the function of ZNRF1 in neuron degeneration, the role of ZNRF1 in innate immunity was unexplored until recently. Our lab recently found that ZNRF1 is a LPS-inducible gene in macrophages [80]. We demonstrated that ZNRF1 mediates polyubiquitination and degradation of caveolin-1 (CAV1), which results in increased Akt-GSK3 β activity upon TLR4 activation. This leads to enhanced the production of pro-inflammatory cytokines and decreased anti-inflammatory cytokine IL-10. Consistently, ZNRF1-deficient mice showed increased resistance to endotoxic and polymicrobial septic shock due to decreased inflammatory response. All in all, ZNRF1 is a novel and positive regulator of the TLR4 signaling pathway through the control of CAV1 protein stability.

Aim



We previously demonstrated that ZNRF1 is a negative regulator of endosomal TLRs-mediated immune response. We also found that ZNRF1 promotes K63-linked polyubiquitination of TLR3 and modulates lysosomal activity, which result in terminating TLR3-mediated signaling in macrophages and MEFs. Moreover, ZNRF1-deficient mice display more resistant to EMCV infection.

Besides TLR3, we previously revealed that ZNRF1 depletion enhances type I interferons but not pro-inflammatory cytokines in pDCs upon activation of TLR7 and TLR9. In line with increased type I interferons production, *ZNRF1*^{-/-} CAL-1 cells exhibit a better defense against HSV-1 infection. In addition, the E3 ubiquitin ligase activity of ZNRF1 is required for its function in TLR7-mediated type I interferons production. However, the detailed mechanism by which ZNRF1 regulates TLR9-mediated immune response, and ZNRF1 is activated upon TLR7/9 activation are still unknown.

In this study, we intended to investigate the underlying mechanism of ZNRF1 regulating TLR7/9-mediated immune response in CAL-1 cells and the activation of ZNRF1 upon TLR7/9 engagement. In addition, we also assessed the physiological function of ZNRF1 in the host against influenza infection *in vivo*.

Material and Methods



Reagents and antibodies

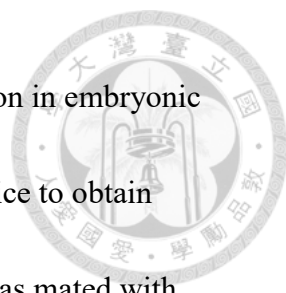
The antibodies used in this study are as follows: anti-ZNRF1 rabbit polyclonal antibody was generated previously in our lab using a synthetic peptide corresponding to residues 71-86 (LYTPASRGTGDSERAP) of human ZNRF1 as an antigen [83]; anti-phospho-IKK α / β (#2697), anti-IKK α (#2682), anti-phospho-AKT (#4060), anti-AKT (#4691), anti-IRAK1 (#4504), anti-phospho-ERK (#4370), anti-ERK (#9102), anti-phospho-p38 (#9211), anti-p38 (#9212), anti-phospho-SAPK/JNK1/2 (#9251), anti-SAPK/JNK1/2 (#9252), anti-p65 (#8242), anti-phospho-STAT1 (#7649), anti-STAT1 (#14994) were purchased from Cell Signaling (Danvers, MA); anti-IkB α (sc-371) and anti-HDAC1 (#sc-7872) were purchased from Santa Cruz (Santa Cruz, CA); anti-GAPDH (#GTX627408) antibody was purchased from GeneTex (Irvine, CA); anti-IRF7 (#ab109255) antibody and anti-IFIT3 (#ab76818) antibody were purchased from Abcam; antibody against α -tubulin (T9026) was obtained from Sigma-Aldrich (St Louis, MO); Brilliant Violet 421 anti-mouse CD45.2 antibody (#109832), PE/Cyanine7 anti-mouse/human CD11b antibody (#101216) and Alexa Fluor® 488 anti-mouse F4/80 antibody (#123120) were purchased from Biolegend; APC anti-mouse CD11c (#17-0114-82) and PE anti-human/mouse CD11b (#50-0112) antibodies were purchased from Thermo Fisher and Tonbo, respectively.



RPMI 1640 (#11875085), Dulbecco's modified Eagle's medium (DMEM, #11965084), Dulbecco's phosphate-buffered saline (DPBS, #21600069), penicillin/streptomycin (P/S, #15140122), sodium pyruvate (#11360070), HEPES (#15630080), glutamax (#35050061), trypsin (#15400054) and L-glutamine (#A2916801) were purchased from Life Technologies (Waltham, MA). Minimum Essential Medium (MEM, #SH30008.02) and fetal bovine serum (FBS, #SH30088.03) were obtained from Hyclone (Logan, UT). Puromycin (#P-600-100) was purchased from Gold Biotechnology. Doxycycline (#D9891), Bovine Serum Albumin (BSA, #A3059), N-p-tosyl-L-phenylalanyl chloromethyl ketone (TPCK)-treated trypsin (#T8802), 2,2,2-Tribromoethanol (Avertin, #AL-T48402), and Tert-Amyl alcohol (#AL-240486) were from Sigma-Aldrich (St Louis, MO). Blasticidin (#ant-bl-1) and ODN2216-FITC (#tlrl-2216f) were purchased from Invivogen (San Diego, CA). R848 (#ALX-420-038-M025) was from Enzo Life Sciences (Farmingdale, NY). CpGA ODN 2216 oligonucleotides was synthesized by Sigma-Aldrich (St Louis, MO) and its sequence is 5'-ggGGGACGATCGTCgggggg-3' (bases shown in capital letters are phosphodiester and those in lower case are phosphorothioate).

Mice

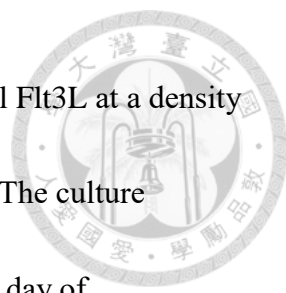
First, *Znrf1*^{F/F} mice were generated via the insertion of two loxP sites in the first



and third introns of the *Znrf1* gene through homologous recombination in embryonic stem cells. *Znrf1*^{F/F} mice were further crossed with Protamine-Cre mice to obtain Protamine-Cre-*Znrf1*^{F/+} mice. Male Protamine-Cre-*Znrf1*^{F/+} mouse was mated with *Znrf1*^{F/F} female mouse to obtain *Znrf1*^{F/-} offspring, which were then backcrossed with C57BL/6 mice to obtain *Znrf1*^{+/-} mice. *Znrf1*^{+/-} mice were further intercrossed to produce *Znrf1*^{+/+}, *Znrf1*^{+/-} and *Znrf1*^{-/-} mice. These mice were maintained in a specific pathogen-free animal facility. All animal experiments were conducted following the animal welfare guidelines and were approved by the Institutional Animal Care and Use Committee (IACUC) of College of Medicine, National Taiwan University (approval no. 20150083).

Preparation of Flt3L-induced bone marrow-derived pDCs (Flt3L-pDCs)

Bone marrow cells were flushed out from femurs and tibiae of 6- to 8-week-old mice with RPMI medium without serum using a 25-gauge syringe. The cells were collected and centrifuged at 800g for 3 min. The cells were resuspended in 1 ml ACK lysis buffer (155 mM NH₄Cl, 10 mM KHCO₃, and 0.1 mM EDTA, pH 7.3) and incubated for 3 min to lyse red blood cells. Cells were then centrifuged at 800g for 3 min to remove ACK lysis buffer, and then resuspended in complete RPMI medium (supplemented with 10% FBS, 100 Units/ml P/S, 1mM sodium pyruvate, 1X L-



glutamine, 1X NEAA and 10 μ l β -ME) supplemented with 100 ng/ml Flt3L at a density of 1×10^6 cells/ml in a 6-well plate and cultured at 37°C in 5% CO₂. The culture medium was replaced with fresh Flt3L-containing medium on the 4th day of differentiation. After 8 days of differentiation, suspension cells (Flt3L-induced bone marrow-derived dendritic cells, herein called Flt3L-BMDCs) were collected, and Flt3L-pDCs were purified using anti-B220 microbeads (Miltenyi Biotec) as described later. Flt3L-pDCs were seeded at a 10^6 cell/ml in a 96-well plate and stimulated with 1 μ g/ml R848 or 3 μ M CpG-A as indicated.

Preparation of Flt3L-pDCs

Flt3L-BMDCs were collected and centrifuged at 1200 rpm for 5 min. The cell pellet was resuspended in 90 μ l staining buffer (DPBS containing 2% FBS) per 10^7 total cells. For per 10^7 cells, 10 μ l CD45R (B220) microbeads were added and mixed well by pipetting. After incubation for 15 min at 4°C, 2 ml of staining buffer per 10^7 cells was added to wash cells. The cells were pelleted by centrifugation at 1200 rpm for 5 min and the cell pellet was resuspended in 500 μ l staining buffer. The cell suspension was then passed through a MACS column placed in the magnetic field of the MACS separator. After washing cells with 500 μ l staining buffer 3 times, the MACS column was removed from the separator and placed on top of a collection tube. The B220

positive cells were then eluted from the MACS column with 1 ml staining buffer.



Cell culture

CAL-1 cells (human pDC cell line) were kindly provided from Dr. Shimeru Kamihiro (Graduate School of Biomedical Sciences, Nagasaki University, Japan). CAL-1 cells were cultured in complete RPMI medium supplemented with 2 mM GlutaMax and 25 mM HEPES. Cells were seeded at a density of 10^6 cells/ml, and incubated at 37°C in 5% CO₂.

Generation of ZNRF1 knockout CAL-1 cells using CRISPR/Cas9 system

The ZNRF1 CRISPR plasmids encoded Cas9 and sgRNA targeting human *ZNRF1* gene were purchased from the National RNAi Core Facility (Academia Sinica, Taiwan).

The targeting sequences for *ZNRF1* were as follows:sg-

1:GATTTTCGGGCACTACCGGAC; sg-2:GCATTTTCGGGCACTACCGGA. In order to

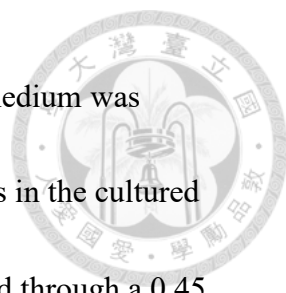
produce lentivirus expressing CRISPR gRNA targeting *ZNRF1*, HEK293T cells were

seeded at a density of 1×10^6 in a 6 cm dish on the day before transfection. 2.5 µg

CRISPR ZNRF1 gRNA plasmids together with 2.25 µg packaging plasmids pCMV-

ΔR8.91 and 0.25 µg envelope plasmid pMD.G were transfected into HEK293T cells by

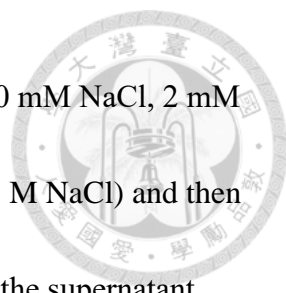
using Turbofect transfection reagent (Thermo Fisher Scientific) according to the



manufacturer's instructions. After incubation for 16 h, the cultured medium was replaced with fresh DMEM medium containing 1% BSA. Lentivirus in the cultured medium were harvested at 48 h and 72 h post-transfection and filtered through a 0.45 μ m filter (Milipore) to remove cell debris. CAL-1 cells seeded at a density of 2×10^5 cells/ml in 6-well plate on the day before infection were incubated with lentivirus-containing medium together with 8 μ g/ml polybrene, and the plate was spun at 1500 rpm for 60 min. After incubation at 37°C overnight, lentivirus-containing medium was replaced with fresh complete RPMI medium and cultured for additional 2 days. CAL-1 cells were then cultured in the selection medium (complete RPMI medium containing 0.5 μ g/ml puromycin) for 1 week. The survived cells were diluted and seeded at single cell per well in 96-well plates. Clones were collected and examined their ZNRF1 expression by immunoblotting. In certain case, *ZNRF1*^{-/-} CAL-1 cells were infected with lentiviruses derived from pAS4.1w.pbsdOn, and grown in the selected medium containing 10 μ g/ml blasticidin for one week. ZNRF1 protein expression in cells was induced by 0.1~0.5 μ g/ml doxycycline 24 h prior to the experiment.

Genomic DNA extraction and sequence alignment

WT and *ZNRF1*^{-/-} CAL-1 cells were collected by centrifugation at 6500 rpm for 2 minutes at 4°C and washed once with ice-cold phosphate-buffered saline (PBS). Cells



were then resuspended 1 ml nuclei lysis buffer (10 mM Tris-HCl, 400 mM NaCl, 2 mM EDTA, 0.5% SDS, pH8.2) and 330 µl protein precipitation buffer (5 M NaCl) and then incubated on ice for 5 min. After centrifugation at 14000g for 5 min, the supernatant was transferred to a new eppendorf tube and equal volume of isopropanol was added to the tube followed by mixing gently by inversion. The solution were then centrifuged at 14000g for 5 min and the pellet were washed with 70% ethanol followed by centrifuged at 14000g for 5 min. The DNA pellets were further air-dried and resuspended in ddH₂O. The genomic DNA was amplified by PCR and subject to sequencing. Sequencing results from WT and *ZNRF1*^{-/-} genomic DNA were aligned by Vector NTI program.

RNA extraction and quantitative RT-PCR (RT-qPCR)

For Flt3L-pDCs, cells were collected in an Eppendorf tube followed by centrifugation at 800g for 3 min. Cell pellets were resuspended in 80 µl Buffer TCL containing 1% β-ME and transferred into a TurboCapture 96 plate containing immobilized oligo-dT. The plate was covered with AlumaSeal II sealing film and incubated overnight at room temperature with gentle shaking. Cell lysates were removed from the plate and the plate was washed with 100 µl Buffer TCW per well three times. cDNA synthesis was performed in the plate using Two-step cDNA synthesis

kit (QIAGEN) with SuperScript™ III reverse transcriptase according to the manufacturer's instructions. 1 µl cDNA was mixed with 9 µl Power SYBR Green PCR Master Mix (Life Technologies) and the amounts of cDNA were measured using StepOne Plus Real-Time PCR System (Applied Biosystems) according to the manufacturer's instructions.

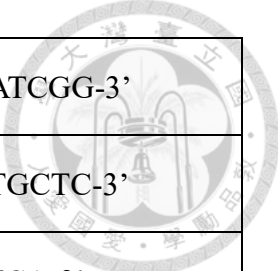
For CAL-1 cells, cells were collected by centrifugation at 6500 rpm for 2 min at 4°C. Cell pellets were resuspended in 500 µl NucleoZOL reagent (MACHEREY-NAGEL) followed by adding 200 µl RNase-free water. The solution was mixed vigorously for 5 seconds and incubated at room temperature for 15 min. The mixtures were centrifuged at 12000g for 15 min at 4°C and the upper aqueous phase was transferred to a new eppendorf tube. An equal volume of 100% isopropanol was added to the solution and mixed gently for seconds to precipitate RNA. The solution was incubated at room temperature for 10 min and centrifuged at 12000g for 10 min at 4°C. RNA pellets were washed with 500 µl 75% ethanol twice, air dried, and resuspended in RNase-free water.

The concentrations of RNAs were determined using Spectrophotometer ND-1000 (NanoDrop). 3000 ng RNA was reverse transcribed into cDNA using the RevertAid H Minus First Strand cDNA Synthesis Kit (Thermo Scientific) according to the manufacturer's instructions. 25 ng cDNA in 2.5 µl DEPC water was mixed with 7.5 µl

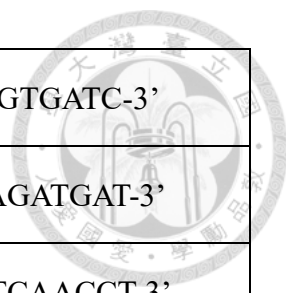
Power SYBR Green PCR Master Mix (Life Technologies) and the cDNA amounts were measured using StepOne Plus Real-Time PCR System (Applied Biosystems) according to the manufacturer's instructions. All qPCR values were normalized to *Cyclophilin* mRNA levels to obtain the relative values. All experiments were performed in triplicate.

Primer sequences for RT-qPCR used in this study were as follows:

Species	Gene	Strand	Sequence
Mice	<i>Ifna4</i>	Forward	5'-CCTGTGTGATGCAGGAACC-3'
		Reverse	5'-TCACCTCCCAGGCACAGA-3'
	<i>Ifnb</i>	Forward	5'-GAAGAGTTACTGCTTTCGCC-3'
		Reverse	5'-CAACAATAGTCTCATTCCACCC-3'
	<i>Il6</i>	Forward	5'-ACAAGAAAGACAAAGCCAGAGTC-3'
		Reverse	5'-ATTGGAAATTGGGGTAGGAAG-3'
	<i>Tnfa</i>	Forward	5'-GTCTACTGAACTTCGGGGTGATC-3'
		Reverse	5'-TCCACTTGGTGGTTTGCTACG-3'
	<i>Il1b</i>	Forward	5'-GAACTCAACTGTGAAATGCCACC-3'
		Reverse	5'-CCACAGCCACAATGAGTGATACT-3'
	<i>Tgfb1</i>	Forward	5'-CGTTACCTTGGTAACCGGCT-3'
		Reverse	5'-GAAAGCCCTGTATTCCGTCTC-3'



	<i>Il10</i>	Forward	5'-TGGGTTGCCAAGCCTTATCGG-3'
		Reverse	5'-ACCTGCTCCACTGCCTTGCTC-3'
	<i>Mcp1</i>	Forward	5'-CTTCTGGGCCTGCTGTTCA-3'
		Reverse	5'-CCAGCCTACTCATTGGGATCA-3'
	<i>Cxcl1</i>	Forward	5'-GCTGGGATTCACCTCAAGAA-3'
		Reverse	5'-CTCCGTTACTTGGGGACAC-3'
	<i>Cxcl2</i>	Forward	5'-AAGTTTGCCTTGACCCTGAA-3'
		Reverse	5'-AGGCACATCAGGTACGATCC-3'
	<i>IAV M</i>	Forward	5'-CTTCTAACCGAGGTCGAAACG-3'
		Reverse	5'-GGCATTTTGGACAAAGCGTCTA-3'
	<i>Cyclophilin</i>	Forward	5'-ATGTGCCAGGGTGGTGACTTT-3'
		Reverse	5'-TTGCCATCCAGCCATTGAGTC-3'
Human	<i>IFNA</i>	Forward	5'-GGCCTTGACCTTTGCTTTACTG-3'
		Reverse	5'-CACAGAGCAGCTTGACTTGCA-3'
	<i>IFNB</i>	Forward	5'-GAAGAGTTACACTGCCTTTGCC-3'
		Reverse	5'-CAACAATAGTCTCATTCCACCC-3'
	<i>IL6</i>	Forward	5'-CTGGTCTTTTGGAGTTTGAGGTAT-3'
		Reverse	5'-GTGGTTGGGTCAGGGGTGGTTAT-3'



	<i>TNFA</i>	Forward	5'-CCTGCTGCACTTTGGAGTGATC-3'
		Reverse	5'-ACTCGGGGTTCGAGAAGATGAT-3'
	<i>CXCL10</i>	Forward	5'-GCATCAGCATTAGTAATCAACCT-3'
		Reverse	5'-ATTGTAGCAATGATCTCAACACG-3'
	<i>OAS1</i>	Forward	5'-TGGGAGCGAGGGAGCAT-3'
		Reverse	5'-CCAAGACCGTCCGAAATCC-3'
	<i>CYCLOA</i>	Forward	5'-AGGTCCCAAAGACAGCAGA-3'
		Reverse	5'-TGTGAAGTCACCACCCTGA-3'

Cell lysates preparation

Cells were collected by centrifugation at 6500 rpm for 2 minutes at 4°C and washed once with ice-cold phosphate-buffered saline (PBS). Cells were then lysed in cell lysis buffer (50 mM Tris HCl pH7.5, 150 mM NaCl, 2 mM EDTA, 1% Triton X-100, 0.5% NP40 and 10% glycerol) supplemented with protease inhibitor cocktail (aprotinin, bestatin, leupeptin and pepstatin), 2 mM dithiothreitol (DTT), 1 mM phenylmethylsulfonyl fluoride (PMSF), 2 mM p-Nitrophenyl Phosphate (pNPP) and 1 mM Na₃VO₄. After incubation on ice for 30 min, cell lysates were sonicated and centrifuged at 13000 rpm for 15 minutes at 4°C. The supernatants were collected and the protein concentrations were determined using the Bradford Protein Assay (Biorad)

following the manufacturer's instructions.



Immunoblotting

Cell lysates were mixed with 1/5 volume of 5X protein sample dye (250 mM Tris-HCl pH6.8, 20% sodium dodecyl sulfate (SDS), 30% glycerol, 16% β -Mercaptoethanol (β -ME), and 0.09% bromophenol blue) and boiled at 95°C for 10 min. The protein samples were separated by SDS-PAGE at constant voltage of 80 volts and transferred to a PVDF membrane at 100 volts for 140 min. The membrane was blocked with TBST (25 mM Tris, 150 mM NaCl, pH7.4, and 0.1% Tween-20) containing 5% non-fat milk for 1 h at room temperature with gentle rotation. For detection of phosphorylated proteins, 5% BSA (Bionovus) in TBST was used for blocking to exclude the contamination of phosphatases. After blocking, the membranes were washed 3 times with TBST for 10 min at room temperature, and then incubated with the indicated primary antibody overnight at 4°C with gentle rotation. The membranes were washed 3 times with TBST for 10 min at room temperature, and then incubated with the HRP-conjugated secondary antibody for 1 h at room temperature. The chemiluminescence signals were detected using Western Lighting Plus-ECL (PerkinElmer) following the manufacturer's instructions and captured by LAS4000 (GE Healthcare).



Ligand internalization assay

CAL-1 cells (3.3×10^5 cells) were seeded in a 96-well plate and stimulated with 2.5 μ M FITC-conjugated ODN 2216 (InvivoGen) for the indicated times at 37°C. 44.6 μ l Trypan blue was added to the well and incubated for 5 min to quench FITC-labeled TLR9 ligand outside the cells. Cells were collected and pelleted at 800g for 3 min. Cell pellets were washed with 500 μ l staining buffer twice and fixed with 200 μ l staining buffer containing 1% paraformaldehyde (PFA), immediately followed by flow cytometric analysis.

Immunoprecipitation

200 μ g HEK293T cell lysates were mixed with 10 μ l Anti-Flag M2 beads (SIGMA A220) and incubated overnight at 4°C with gentle rotation. The beads were then centrifuged at 8000 rpm for 3 min at 4°C and washed three times with ice-cold cell lysis buffer (50 mM Tris HCl pH7.5, 150 mM NaCl, 2 mM EDTA, 1% Triton X-100, 0.5% NP40 and 10% glycerol) supplemented with protease inhibitor. The immunoprecipitants were resuspended in 50 μ l cell lysis buffer and 1/5 volume of 5X protein sample dye and boiled at 95°C for 10 minutes. The mixtures were then centrifuged at 8,000 rpm for 3 min and the supernatants were subject to SDS-PAGE for immunoblotting analysis.

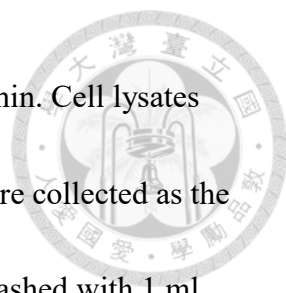


Ubiquitination assay

Cells were lysed with cell lysis buffer (50 mM Tris HCl pH7.5, 150 mM NaCl, 2 mM EDTA, 1% Triton X-100, 0.5% NP40 and 10% glycerol) supplemented with protease inhibitor and 20 mM N-Ethylmaleimide (NEM). 200 µg cell lysates were mixed with 0.2 µg anti-GFP antibody (Santa Cruz sc-9996) and incubated overnight at 4°C with gentle rotation. 10 µl of 50% Protein-A slurry beads were added to the samples and incubated at 4°C for 2 h with gentle rotation. The beads were centrifuged at 8,000 rpm for 3 min at 4°C and washed three times with ice-cold cell lysis buffer supplemented with protease inhibitor. The immunoprecipitants were resuspended in 50 µl cell lysis buffer and 1/5 volume of 5X protein sample dye and boiled at 95°C for 10 minutes. The mixtures were then centrifuged at 8,000 rpm for 3 min and the supernatants were subject to SDS-PAGE for immunoblotting analysis.

Cytosolic and nuclear extract fractionation

CAL-1 cells (8×10^6 cells) were pelleted in a 15 ml centrifuge tube at 6,500 rpm for 2 min. The cell pellet was resuspended in 1 ml cold PBS and transferred to an eppendorf tube, followed by centrifugation at 6500 rpm for 2 min. The cells were then lysed with 200 µl nuclear fractionation buffer A (10 mM HEPES, 1.5 mM MgCl₂, 10 mM KCl, 0.5 mM DTT, 0.05% NP40 pH7.9) containing 1X protease inhibitor cocktail



(aprotinin, bestatin, leupeptin, and pepstatin) and kept on ice for 10 min. Cell lysates were pelleted at 3000 rpm for 10 min at 4°C, and the supernatants were collected as the cytosolic fraction. The remaining nuclei pellets were subsequently washed with 1 ml nuclear fractionation buffer A three times and pelleted at 13,000 rpm for 1 second at 4°C. The pellets were lysed with 50 µl nuclear fractionation buffer B (5 mM HEPES, 1.5 mM MgCl₂, 0.2 mM EDTA, 0.5 mM DTT, 26% glycerol, and 300 mM NaCl) containing 1X protease inhibitor cocktail and subjected to sonication (Branson Sonifier 250 Analog Ultrasonic Homogenizer, Cat. #N468) using the duty cycle control of 20% setting and output control setting of 5 for 3 seconds, followed by incubation on ice for 10 min. The nuclear lysates were centrifuged at 13000 rpm for 15 min at 4°C and the supernatants were collected as the nuclear fraction.

Virus amplification

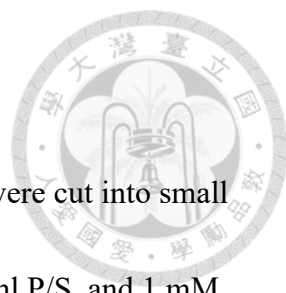
Influenza A (H5N1, strain A/Vietnam/1203/04) was kindly provided by Dr. Hui-Ling Yen (Centre of Influenza Research, School of Public Health, The University of Hong Kong, Hong Kong). This strain is a vaccine seed strain with multibasic HA cleavage site replaced by that of a low-pathogenicity avian influenza virus [102]. In each well of 6 well plate, 10⁶ Madin-Darby Canine Kidney cells (MDCK) cells were seeded and infected with influenza A at an MOI of 0.01 in 1 ml serum-free MEM

medium supplemented with 100 Units/ml P/S and 2 μ g/ml TPCK-treated trypsin, followed by incubation for 2 h at 37°C for adsorption. 3 ml serum-free MEM medium supplemented with 100 Units/ml P/S and 2 μ g/ml TPCK-treated trypsin was added to each well of the plate and incubated for another 2 days. When most cells displayed a cytopathic effect (CPE) characterized by cell rounding, cultured medium was collected and centrifuged at 1500 rpm for 10 min. Virus-containing supernatants were aliquoted and stored at -80°C.

Intratracheal instillation

Mice were anesthetized by injecting intraperitoneally 260 μ l avertin (25mg/ml). Anesthetized mice were placed on surgical board and fixed by stickers. A small incision was made near the anterior aspect of the neck. Platysma and anterior tracheal muscles were dissected away to visualize the tracheal rings. 50 μ l H5N1 virus were injected into the trachea by using a 29-gauge needle. The needle and syringe were holded parallel with the trachea. The gasping response of the mice following the instillation of virus into the lungs was used as an indicator of successful processing. The wound was sutured and the skin was applied with povidone-iodine solution.

Infiltrating cells isolation



Mouse lung tissues were collected and weighted. Lung tissues were cut into small pieces in 200 µl of RPMI complete medium (10% FBS, 100 Units/ml P/S, and 1 mM sodium pyruvate) and transferred to 5 ml of RPMI complete medium containing 0.167 mg/ml of Liberase TM (Roche) in a 15 ml tube. The tissue was homogenized by passing through a 24-gauge syringe three times followed by centrifugation at 300g for 5 min. The cell pellets were resuspended in 4 ml of 45% percoll, which was over 3 ml of 81% percoll. After centrifugation at 1,500g for 20 min without brake, cells at the interface were collected and transferred to a 15 ml tube containing 8 ml DPBS followed by centrifugation at 1,000g for 5 min. The cell pellets were resuspended in 1 ml DPBS and centrifuged at 800g for 3 min. Cells were resuspended in 400 µl of staining buffer (DPBS containing 2% FBS). 100 µl of cell suspension was stained with antibodies specific against CD45.2, CD11c, B220 and siglec-F for pDCs, or CD45.2, CD11b, F4/80 and Ly6G for neutrophils. Another 100 µl of cell suspension was left unstained. Cells were incubated with antibodies on ice for 15 min and washed twice with cold staining buffer. Stained and unstained cells were subjected to flow cytometry analysis immediately to quantify the number of specific cell populations (total cell count = cell count \times 4/tissue weight \times whole organ weight).

Statistical analysis

In vitro results were presented as mean \pm SD and *in vivo* results were presented as mean \pm SEM. Statistical significances between two groups were determined by the two-tailed Student's t-test. *P<0.05, **P<0.01, ***P<0.001.



Results

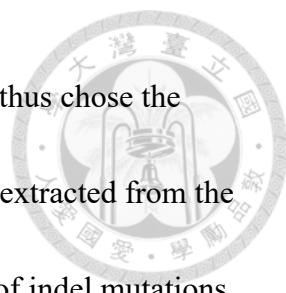


ZNRF1 depletion in Flt3L-pDCs enhances the production of type I IFNs and pro-inflammatory cytokines upon TLR7 and TLR9 activation

To confirm the regulatory role of ZNRF1 in TLR7- and TLR9-mediated immune response, Flt3L-pDCs from *Znrf1*^{+/+} and *Znrf1*^{-/-} mice were stimulated with TLR7 (R848) or TLR9 (CpGA) ligands. *Znrf1*^{-/-} pDCs produced higher amounts of type I IFNs and pro-inflammatory cytokines in response to TLR7 or TLR9 ligands (Figure 1 and 2), confirming that ZNRF1 is a negative regulator of TLR7- and TLR9-induced type I IFNs production.

ZNRF1 depletion promotes increased amount of type I IFNs in CAL-1 upon TLR7 activation

To further investigate the mechanism by which ZNRF1 regulates TLR7- and TLR9-mediated immune responses, we utilized a human pDC cell line, CAL-1. Previous studies have shown that the blastic plasmacytoid dendritic cell neoplasm (BPDCN)-derived CAL-1 cells display similar phenotypes and functions as freshly isolated human pDCs [81]. When stimulated with TLR7 (R848) or TLR9 (CpGA) ligands, CAL-1 cells produce large amounts of type I interferons such as IFN- β [82,83]. We generated *ZNRF1*^{-/-} CAL-1 cells using CRISPR/Cas9 system, and obtained several



clones whose ZNRF1 level was significant reduced (Figure 3A). We thus chose the sgZNRF1#2 (2) clone for the following experiments. Genomic DNA extracted from the sgZNRF1#2 (2) clone was subjected to sequencing and the presence of indel mutations was confirmed (Figure 3B). Consistent with the results in Flt3L-pDCs, our results demonstrated that *ZNRF1*^{-/-} CAL-1 cells produced more type I IFNs levels compared to WT cells upon R848 (Figure 4).

Interestingly, the mRNA expression of pro-inflammatory cytokines was increased in *ZNRF1*^{-/-} CAL-1 cells compared to WT cells after R848 stimulation (Figure 4).

ZNRF1 depletion enhances IKK α activation and nuclear translocation of IRF7 upon TLR7 activation in CAL-1 cells.

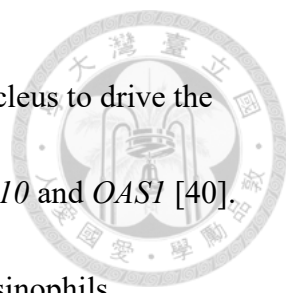
TLR7 and TLR9 are synthesized in the ER, and trafficked to the endosomes with the aid of chaperone protein UNC93B1. Following the cleavage of TLR7 and TLR9 and ligands engagement, the adaptor protein MyD88 is recruited to the receptor and formed the Myddosome complex, which further induces two major signaling pathways: IRF7 signaling and NF- κ B signaling. Thus, we speculated that ZNRF1-mediated TLR7 and TLR9-induced type I interferons production may be through regulating the IRF7 signaling pathway.

It has been known that upon TLR7/9 activation, transcription factor IRF7 is

phosphorylated by IRAK1 or IKK α and then translocates into the nucleus to drive type I interferons production in pDCs. Several reports demonstrated that loss of IKK α or IRAK1, or inhibition of PI3K impaired type I interferons production upon TLR7 and TLR9 activation, suggesting the involvements of these molecules in TLR7- and TLR9-induced type I IFNs production [84-86].

Our data showed that ZNRF1 regulated the production of type I IFNs upon TLR7 and TLR9 activation. To further investigate which step ZNRF1 affects TLR7- and TLR9-mediated type I IFNs production, we carried out immunoblotting to examine the activation of IKK α , IRAK1 and AKT upon TLR7 and TLR9 activation in WT and *ZNRF1*^{-/-} CAL-1. The phosphorylation of IKK α , which represents its activation, was significantly increased in *ZNRF1*^{-/-} CAL-1 upon TLR7 activation (Figure 5). However, the phosphorylation at serine 473 of AKT, the main downstream protein of PI3K activation, was decreased in *ZNRF1*^{-/-} CAL-1 upon TLR7 activation (Figure 5). In addition, the degradation of IRAK1 was not affected by ZNRF1 depletion (Figure 5). Next, we performed subcellular fractionation to assess the cellular localization of IRF7 in CAL-1 cells in response to TLR7 ligands. Our results reveal that the nuclear translocation of IRF7 was increased in *ZNRF1*^{-/-} CAL-1 upon R848 treatment (Figure 6)

Once type I IFNs are secreted, they can bind to type I interferon receptor (IFNAR) via autocrine and paracrine manners to activate the downstream JAK/STAT signaling



cascades. STAT1 is then phosphorylated and translocated into the nucleus to drive the expression of numerous IFN-stimulated genes (ISGs), such as *CXCL10* and *OAS1* [40]. *CXCL10* are inflammatory chemokines which can recruit T cells, eosinophils, monocytes and NK cells to the site of infection [87]. *OAS1* encodes 2'-5'-Oligoadenylate synthetase 1, which can activate latent cellular RNase L to degrade single-stranded viral RNA, thereby suppressing viral propagation [88]. Thus, we performed immunoblotting to examine STAT1 phosphorylation and RT-qPCR to detect the mRNA expression of several ISGs upon stimulation with R848. Our data showed that the phosphorylation of STAT1 was increased in TLR7-activated *ZNRF1*^{-/-} CAL-1 cells. In line with STAT1 activation, the expression of *CXCL10* and *OAS1* were enhanced in *ZNRF1*^{-/-} CAL-1 upon TLR7 activation (Figure 7). To test whether ZNRF1 directly regulates type I IFN-mediated signaling pathway and further affects the production of ISGs, we performed immunoblotting to examine STAT1 phosphorylation and IFIT3 expression upon IFN β stimulation. Our results showed that there was no significant difference in the phosphorylation of STAT1 between WT and *ZNRF1*^{-/-} CAL-1 cells after IFN β stimulation (Figure 8A). In addition, the expression of IFIT3 was slightly decreased in *ZNRF1*^{-/-} CAL-1 cells after IFN β stimulation (Figure 8B). Taken together, ZNRF1 is not involved in type I IFN-mediated response, thus excluding a possibility that ZNRF1-mediated TLR7- and TLR9-driven immune response through

direct modulation of type I IFN-triggered signaling.

All in all, ZNRF1 regulates IKK α activation to modulate type I IFNs and subsequent ISG expression in pDCs upon TLR7 activation.



ZNRF1 depletion promotes TLR7-induced MAPK and IKK β /NF- κ B activation in CAL-1 cells.

In TLR7- and TLR9-triggered NF- κ B pathway, the Myddosome complex activates the TAK1 complex composing TAK1 and TAB1/2, which further induces the activation of MAPKs and IKK β /NF- κ B, leading to the production of pro-inflammatory cytokines [38]. We therefore also examined the activation of NF- κ B signaling by immunoblotting. Our results showed that the phosphorylation of MAPKs, including JNK, ERK and p38, and I κ B degradation, which represents the activation of the canonical IKK β /NF- κ B pathway, were increased in *ZNRF1*^{-/-} CAL-1 after R848 stimulation (Figure 9).

ZNRF1 Y103 residue is important for its regulatory function in TLR7 signaling

It remains unknown how ZNRF1 is activated upon TLR7 and TLR9 engagement. Previous studies reported that ZNRF1 was activated by epidermal growth factor receptor (EGFR) through phosphorylation at its Y103 residue upon oxidative stress which is critical for neuronal apoptosis and axonal degeneration during Wallerian

degeneration [90]. In addition, EGFR was demonstrated to be required for TLR3/4/9 signaling [89-91]. We therefore speculated that ZNRF1 is activated by EGFR by phosphorylation of its Y103 residue.



To investigate whether phosphorylation at Y103 of ZNRF1 is involved TLR7- and TLR9-triggered immune responses, we first reconstituted *ZNRF1*^{-/-} CAL-1 with inducible WT ZNRF1 or the phospho-deficient mutant ZNRF1 (Y103F). CAL-1 cells reconstituted with WT ZNRF1 and ZNRF1 (Y103F) were stimulated with 0.5 µg/ml doxycycline for 24 h prior to the experiments to induce ZNRF1 protein expression (Figure 10A). *ZNRF1*^{-/-} CAL-1 cells reconstituted with WT ZNRF1, but not in those reconstituted with vector or phospho-deficient mutant ZNRF1 (Y103F), displayed decreased activation of IKKα, AKT and MAPK after R848 stimulation (Figure 10B and 10C). Thus, ZNRF1 Y103 residue is critical for TLR7-mediated signaling. However, it remains to be further investigated whether ZNRF1 Y103 residue is phosphorylated upon TLR7 activation and which kinase is responsible for its phosphorylation.

ZNRF1 depletion promotes increased amount of type I IFNs in CAL-1 upon TLR9 activation.

Consistent with the results in Flt3L-pDCs, our results demonstrated that *ZNRF1*^{-/-}

CAL-1 cells produced more type I IFNs production compared to WT cells upon CpGA stimulation (Figure 11). Interestingly, there was no significant difference on the level of pro-inflammatory cytokines between WT and *ZNRF1*^{-/-} CAL-1 in response to CpGA (Figure 11).

***ZNRF1* depletion enhances IKK α activation and nuclear translocation of IRF7 but has little impact on MAPK activation upon TLR9 activation in CAL-1 cells.**

Similar to the results of TLR7 signaling, phosphorylation of IKK α and the nuclear translocation of IRF7 were increased in *ZNRF1*^{-/-} CAL-1 upon CpGA treatments (Figure 12 and 13). In addition, phosphorylation of STAT1 and further the mRNA expression of ISGs such as *CXCL10* and *OAS1* were enhanced in *ZNRF1*^{-/-} CAL-1 upon TLR9 activation (Figure 14). Unlike the results in TLR7 signaling, there was no significant difference on MAPKs activation between WT and *ZNRF1*^{-/-} CAL-1 after CpGA stimulation (Figure 15), indicating that *ZNRF1* regulates TLR7, but not TLR9-induced NF- κ B signaling.

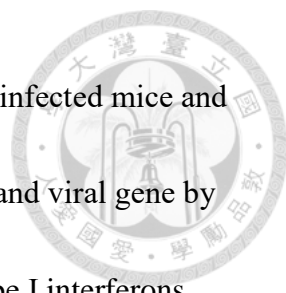
ZNRF1 Y103 residue is important for its regulatory function in TLR9 signaling



To investigate whether phosphorylation at Y103 of ZNRF1 is also involved TLR9-triggered immune responses, we reconstituted *ZNRF1*^{-/-} CAL-1 with inducible WT ZNRF1 or the phospho-deficient mutant ZNRF1 (Y103F). CAL-1 cells reconstituted with WT ZNRF1 and ZNRF1 (Y103F) were stimulated with 0.5 µg/ml doxycycline for 24 h prior to the experiments to induce ZNRF1 protein expression (Figure 16A). *ZNRF1*^{-/-} CAL-1 cells reconstituted with WT ZNRF1, but not in those reconstituted with vector or phospho-deficient mutant ZNRF1 (Y103F), displayed decreased activation of IKKα and AKT after CpGA stimulation (Figure 16B and 16C). Thus, ZNRF1 Y103 residue is also critical for TLR9-mediated signaling.

ZNRF1 deficient mice are resistant to H5N1 influenza A virus infection.

Type I IFNs production is crucial for the host to defend viral infection. Since we showed that ZNRF1 depletion in CAL-1 enhanced type I interferons production, we examined the importance of ZNRF1 in antiviral responses *in vivo*. We intratracheally delivered H5N1 influenza A virus into the distal lung of mice and monitored the survival of wild type and *Znrf1*^{-/-} mice daily for 14 days. Our results showed that ZNRF1 deficient mice displayed a better survival rate compared to WT mice (Figure



17). In addition, we harvested the lung tissues from naïve and H5N1 infected mice and analyzed the mRNA expression of different inflammatory cytokines and viral gene by RT-qPCR at day 6 post-infection. We found that reduced levels of type I interferons, pro-inflammatory cytokines, anti-inflammatory cytokines, chemokines and the mRNA expression of viral gene were observed in lungs from *Znrf1*^{-/-} mice (Figure 18). To investigate lung immune cell populations at day 6 after infection, we digested lung tissues with Liberase TM to prepare a single cell suspension and then stained cells with antibodies against specific markers followed by flow cytometry. Our results showed that ZNRF1 deficient mice had decreased numbers of alveolar macrophages, conventional DCs and neutrophils in lungs at day 6 after infection (Figure 19), suggesting that less immune cells were recruited to the infection site. Our animal results suggest two possible roles of ZNRF1 in the host during IAV infection: 1. During the early phase of H5N1 infection, ZNRF1 may suppress type I IFN production in pDCs; 2. ZNRF1 may affect immunopathology by regulation of inflammatory mediators production. Nevertheless, the exact physiological effects of ZNRF1 in the host against IAV infection needs to be further investigated in the future.

Discussion

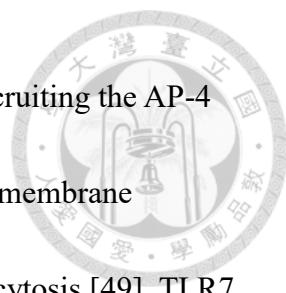


Endosomal TLRs recognize PAMPs or DAMPs and then trigger a series of intracellular signaling events leading to upregulation of cytokines and type I IFNs involved in inflammatory responses. However, this process needs to be tightly controlled to avoid excess inflammation which results in autoimmune or inflammatory diseases [11].

In this study, we demonstrated that the E3 ubiquitin ligase ZNRF1 is a negative regulator of TLR7- and TLR9-mediated immune response. Our *in vitro* results showed that ZNRF1 depletion increased IKK α activation and nuclear translocation of transcription factor IRF7, leading to increased type I IFNs production and further ISG expression after TLR7 and TLR9 activation. Moreover, Y103 residue of ZNRF1 is critical for TLR7- and TLR9-mediated signaling pathway. In addition, our results showed that ZNRF1-deficient mice are resistant to H5N1 Influenza virus infection.

The possible role of ZNRF1 in TLR7 and TLR9 trafficking

Previous studies showed that the localization of TLR7 and TLR9 is crucial for the recruitment of distinct downstream signaling proteins leading to the induction of either pro-inflammatory cytokines or type I IFNs expression. Upon stimulation with ligands, TLR7 and TLR9 traffic from the endoplasmic reticulum (ER) to the endosome through



different mechanisms. TLR7 directly traffics to the endosomes by recruiting the AP-4 complex, a sorting complex, whereas TLR9 transports to the plasma membrane followed by translocating to the endosomes via AP-2-mediated endocytosis [49]. TLR7 and TLR9 encountered their ligands at the early endosomes, where they induce the transcription of pro-inflammatory genes via activation of NF- κ B. Later, TLR7 and TLR9 together with their ligands are transported to the lysosome-related organelles (LROs), also called IRF7 endosome, and turn on type I IFNs production [91]. Our results showed that ZNRF1 deficiency enhanced type I IFNs and pro-inflammatory cytokines after TLR7 activation (Figure 4), suggesting that ZNRF1 may control both TLR7 entry into and exit from the LROs. By contrast, ZNRF1 deficiency enhanced type I IFNs but not pro-inflammatory cytokines after TLR9 activation (Figure 11), suggesting that ZNRF1 may regulate TLR9 export from the LROs. However, the dynamic trafficking of TLR7 and TLR9 from the early endosomes to the lysosomes should be carefully monitored in control and ZNRF1-deficient cells upon ligand treatments in the future, so that we can figure out how ZNRF1 regulates TLR7 and TLR9 trafficking and their downstream signaling (Figure 20).

Because no good TLR7 antibody for the immunofluorescence staining is currently available, it's difficult to monitor TLR7 trafficking directly using the immunofluorescence technique. Thus, we constructed a lentivirus with AcGFP fused to

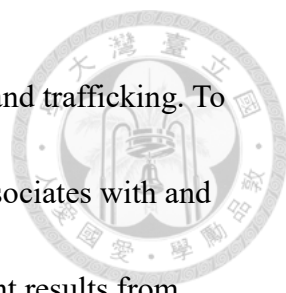
the C-terminus of TLR7 to ensure the TLR7-AcGFP fusion protein is intact after undergoing proteolytic cleavage. Unfortunately, this construct is too big to be packaged into lentiviruses based on the results of flow cytometry analysis that almost 100%



CAL-1 cells were successfully infected with lentivirus expressing AcGFP, whereas less than 8% cells expressed TLR7-AcGFP. We also tried other transfection reagents, such as DOTAP, TransIT and Turbofect, but they all failed to deliver this construct DNA into CAL-1 cells. In the future, we will try to deliver the DNA construct into CAL-1 cells using electroporation. Alternatively, we recently obtained a knockin mice expressing TLR7 fused with HA tag from prof. Yi-Ping Hsueh at the Institute of Molecular Biology, Academia Sinica. We will generate pDCs from bone marrow cells of TLR7-HA knock-in mice and assess the trafficking of TLR7 using the immunofluorescence staining.

The possible role of ZNRF1 in ubiquitination of TLR7/9

Our previous studies showed that the E3 ubiquitin ligase ZNRF1 promotes caveolin-1 ubiquitination and degradation to modulate TLR4-mediated immune responses [80]. In this study, we showed that ZNRF1 controls the trafficking of TLR7 and TLR9 to modulate their downstream signaling. It has been shown that ubiquitination is crucial for the intracellular trafficking of the receptor. Thus, we



speculate that ZNRF1 may regulate TLR7 and TLR9 ubiquitination and trafficking. To address this possibility, we will examine whether ZNRF1 directly associates with and ubiquitinates TLR7 and TLR9. In addition, according to the alignment results from UniProt website, K953 of TLR7 and K932 of TLR9 are conserved lysine residues among human and mouse. We will mutate these conserved lysine residues to arginine on TLR7 and TLR9 by site-directed mutagenesis and assess whether ZNRF1 is not able to ubiquitinate these mutant TLRs and these mutant TLRs can promote type I IFNs expression.

The possible role of phosphorylation at Y103 of ZNRF1 in TLR7- and TLR9-induced signaling pathway

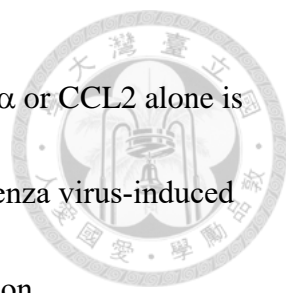
Previous study showed that ZNRF1 was activated by EGFR via phosphorylation at its Y103 residue during oxidative stress, which results in proteasomal degradation of AKT and GSK3B activation, leading to Wallerian degeneration [92]. Another study demonstrated that the epidermal growth factor receptor ErbB1 and Src phosphorylate the two tyrosine residues of TLR3 to recruit the adaptor protein TRIF and initiate downstream signaling [89]. In addition, EGFR kinase activity is required for TLR4 signaling [90]. Thus, we speculate that ZNRF1 may be phosphorylated and activated by EGFR and further regulates TLR7- and TLR9-mediated signaling.

The possible role of ZNRF1 during H5N1 influenza virus infection



Type I IFNs play an important role in antiviral host defense system. Type I IFN can bind to type I interferon receptor to induce the expression of numerous interferon-stimulated genes (ISGs), including the Mx proteins, double-stranded RNA-activated protein kinase R (PKR) and 2',5'-oligoadenylate synthetase (OAS), all of which can enhance viral RNA degradation and suppress virus proliferation. Previous studies demonstrated that the nonstructural protein 1 (NS1) of influenza virus is a vital virulence factor in different animal models due to its suppressive effect on the antiviral functions of type I IFNs [94, 95]. Notably, there is considerable variation among influenza virus strains [96]. It was reported that mice lacking type I IFN- α/β receptor signaling displayed susceptible to both highly (A/Hong Kong/483/97) and low (A/Hong Kong/486/97) pathogenic H5N1 influenza viruses, suggesting that the IFN- α/β -mediated immune responses provide some degree of protection for the host at the early stage of H5N1 infection [97]. In addition, Mx1 protein protects mice from the infection of high virulence of A/Vietnam/1203/04 (H5N1) virus through inhibition of viral RNA polymerase, resulting in reduced viral growth and dissemination [98].

We observed that the levels of pro-inflammatory cytokines including IL-6, TNF- α and CC chemokine ligand 2 (CCL2) were elevated during H5N1 virus infection. It has been widely hypothesized that the 'cytokine storm' is the main cause of mortality for



influenza viral infection [99]. Interestingly, deficiency of IL-6, TNF- α or CCL2 alone is not sufficient to protect mice from A/Vietnam/1203/04 (H5N1) influenza virus-induced mortality [100]. Moreover, mice treated with glucocorticoid, a common immunosuppressive drug, did not show reduced mortality after challenge with A/Vietnam/1203/04 (H5N1) influenza virus [100, 101]. Taken together, inhibition of viral replication at the early stage is more effective than suppression of cytokine production to protect the host against A/Vietnam/1203/04 (H5N1) influenza virus infection.

Our results showed that ZNRF1 deficient mice were resistant to H5N1 influenza A virus infection. In addition, ZNRF1-deficient mice recruited decreased numbers of immune cells and produced less cytokines in lungs at day 6 after IAV infection. There are two possible roles of ZNRF1 during IAV infection: 1. At the early phase of H5N1 infection, ZNRF1 may suppress type I IFN production in pDCs; 2. ZNRF1 may control the host's immunopathology by regulating the production of inflammatory mediators. Nevertheless, the exact physiological role of ZNRF1 in the host against IAV infection needs to be further investigated in the future.

Figures

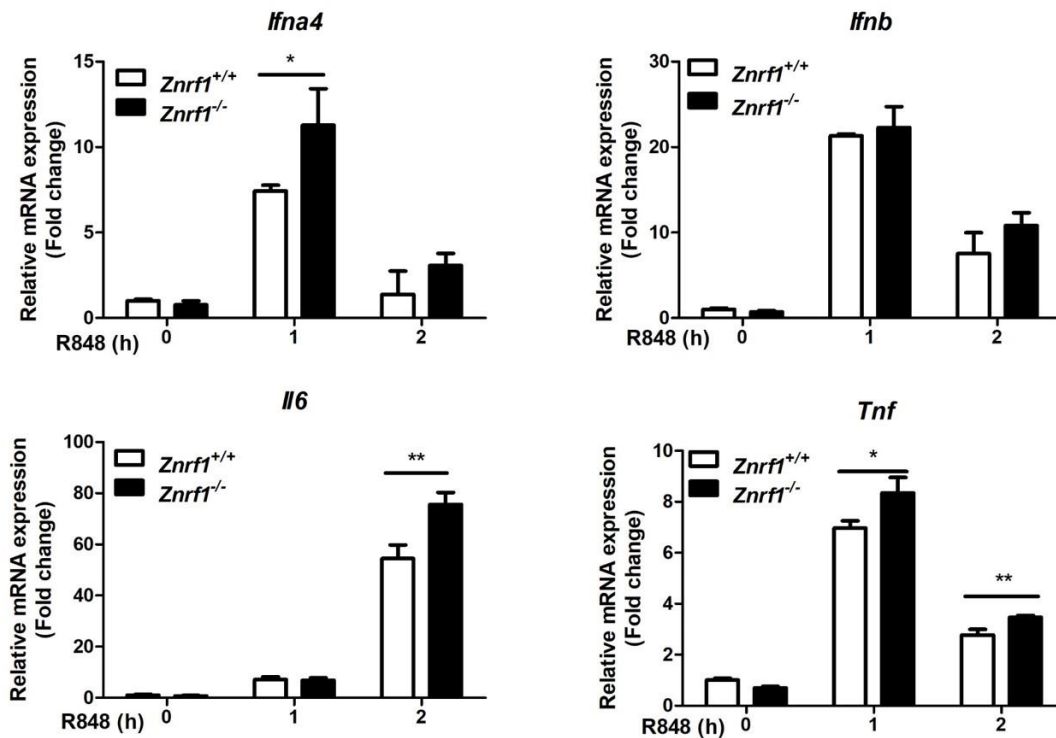


Figure 1. ZNRF1 depletion enhances TLR7-triggered type I IFNs and pro-inflammatory cytokines in Flt3L-pDCs. Bone marrow harvested from *Znrfl*^{+/+} and *Znrfl*^{-/-} mice were cultured with 100 ng/ml hFlt3L for 8 days and selected by anti-B220 microbeads to collect pDCs. Flt3L-pDCs were stimulated with 1 µg/ml R848 for the indicated times. The mRNA expression of indicated genes were analyzed by RT-qPCR and the qPCR values were normalized to *Cyclophilin* level. *P<0.05, **P<0.01, ***P<0.001 (Student's *t*-test)

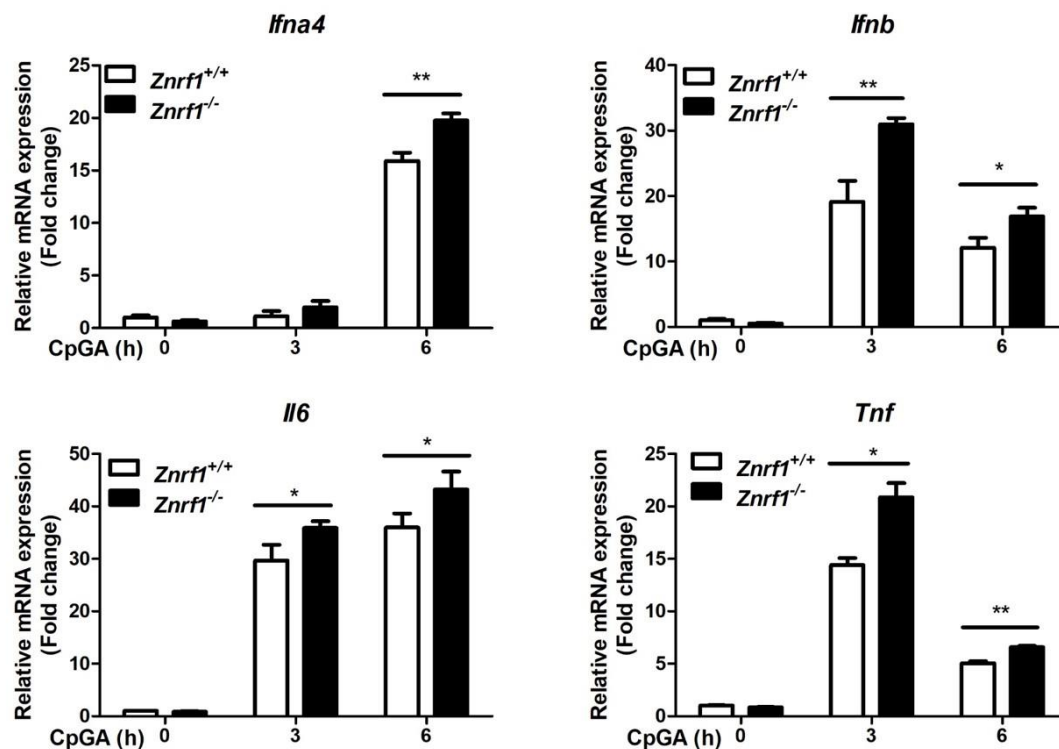


Figure 2. ZNRF1 depletion enhances TLR9-triggered type I IFNs and pro-inflammatory cytokines in Flt3L-pDCs. Bone marrow harvested from *Znrfl*^{+/+} and *Znrfl*^{-/-} mice were cultured with 100 ng/ml hFlt3L for 8 days and selected by anti-B220 microbeads to collect pDCs. Flt3L-pDCs were stimulated with 3 μ M CpGA for the indicated times. The mRNA expression of indicated genes were analyzed by RT-qPCR.

*P<0.05, **P<0.01, ***P<0.001 (Student's *t*-test)



(A)



(B)

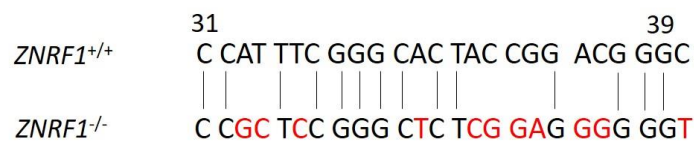


Figure 3. Generation of *ZNRF1*^{-/-} CAL-1 cells by CRISPR/Cas9 system. CAL-1

cells were infected with lentivirus containing plasmid encoded for sgRNA targeting human *ZNRF1* gene. After selection with 0.5 µg/ml puromycin for 5 days, single cell was seeded in 96-well plates. (A) Cells were collected from each individual clones and cell lysates were prepared for analyzing ZNRF1 protein level by immunoblotting. *sgZNRF1*#2 (2) clone was chosen for the following experiments. (B) Genomic DNAs were extracted from control and *ZNRF1*^{-/-} CAL-1 cells and the region surrounding the targeted site was amplified by PCR for sequencing. Indel mutations are indicated in red.

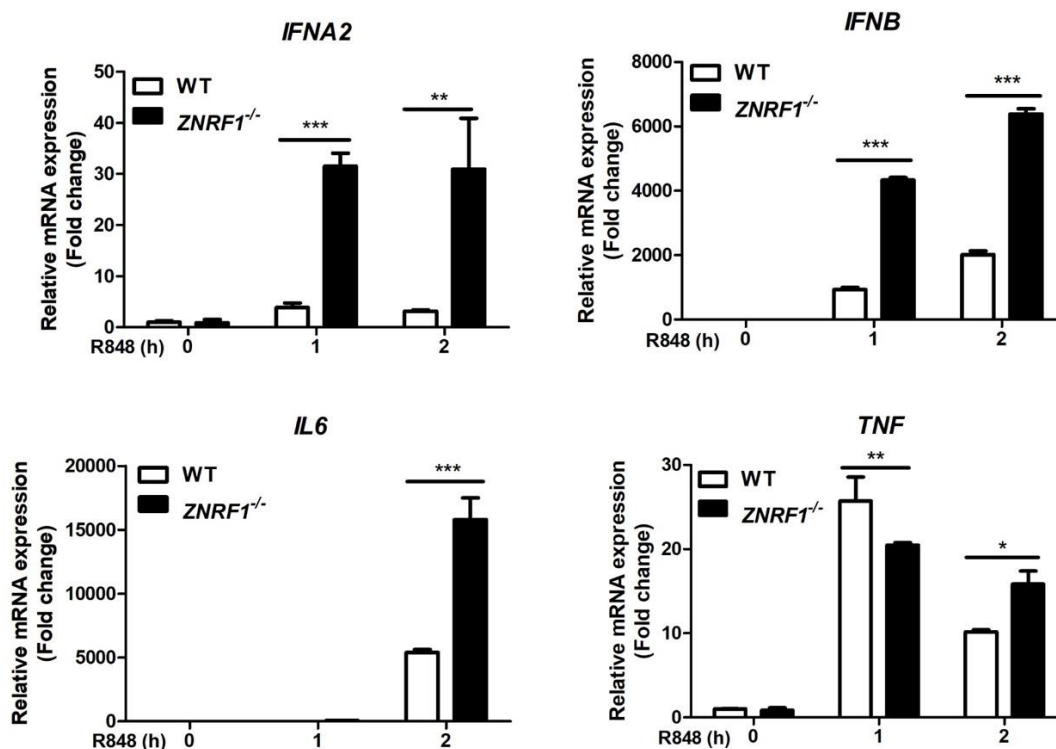


Figure 4. Depletion of ZNRF1 enhances TLR7-induced type I IFNs and pro-inflammatory cytokines in CAL-1 cells. WT and *ZNRF1*^{-/-} CAL-1 cells were stimulated with 1 μg/ml R848 for the indicated times. The mRNA expression of indicated genes were analyzed by RT-qPCR. *P<0.05, **P<0.01, ***P<0.001 (Student's *t*-test). The data are representative of three independent experiments performed in triplicate (error bars, s.d.).

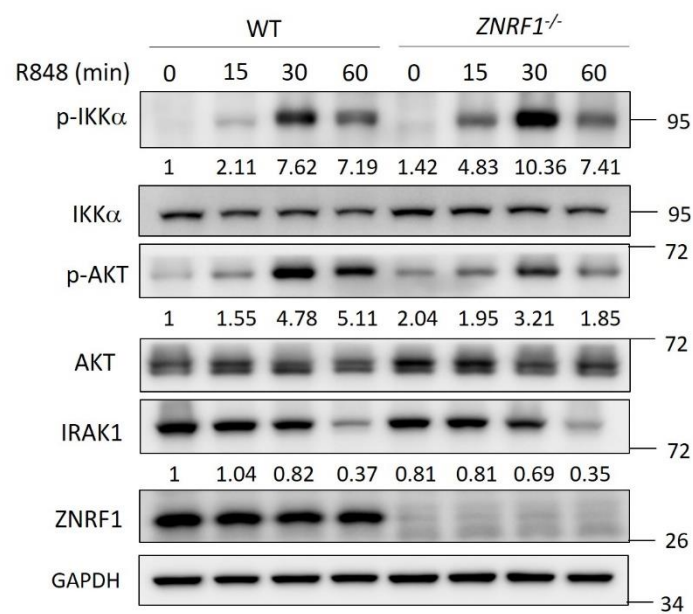


Figure 5. ZNRF1 deficiency enhances IKKα activation in CAL-1 cells after stimulation with R848. WT and *ZNRF1*^{-/-} CAL-1 cells were stimulated with 1 μg/ml R848 for the indicated times. Cell lysates were collected and immunoblotted with the indicated antibodies. The intensities of p-IKKα and p-AKT signals are expressed as fold induction compared to the untreated wild type cells after normalized to their unphosphorylated forms. The intensity of IRAK1 signal is expressed as fold induction compared to the untreated wild type cells after normalized to the internal control GAPDH. The data are representative of four independent experiments.

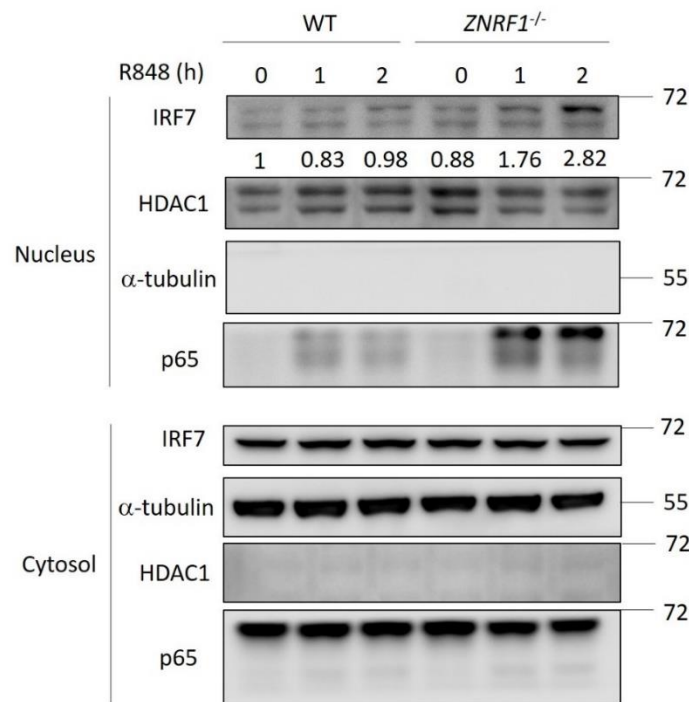
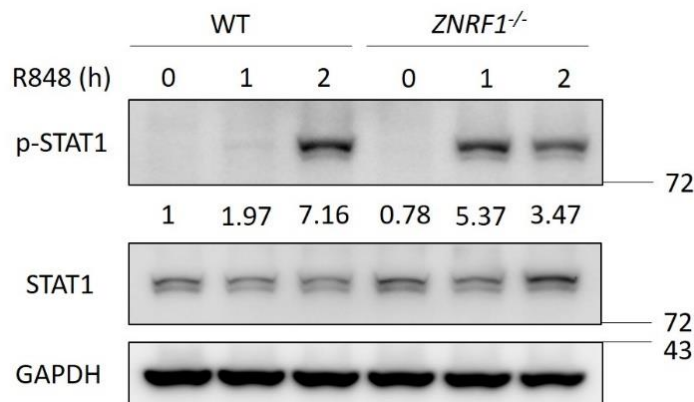


Figure 6. *ZNRFI* deficiency increases IRF7 activation in CAL-1 cells after stimulation with R848. WT and *ZNRFI*^{-/-} CAL-1 cells were stimulated with 1 μg/ml R848 for the indicated times. Cells were collected and subjected to the subcellular fractionation to obtain the cytosolic and nuclear fractions followed by immunoblotted with the indicated antibodies. HDAC1 and α-tubulin serve as the markers for the nuclear and cytosolic fractions, respectively. The data are representative of three independent experiments.



(A)



(B)

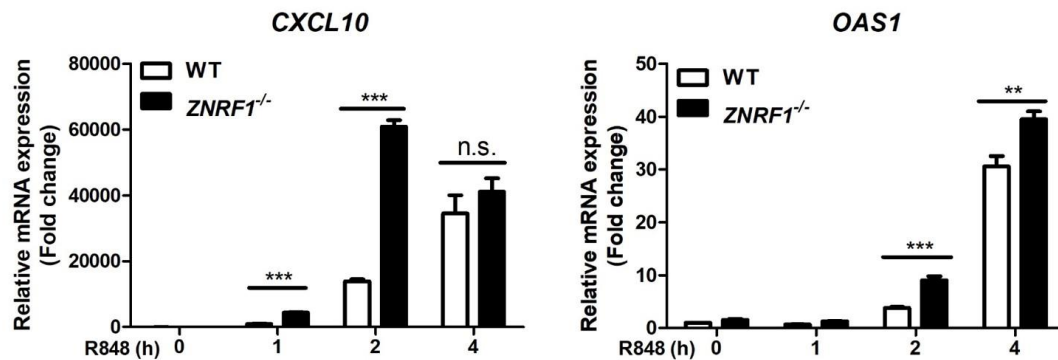


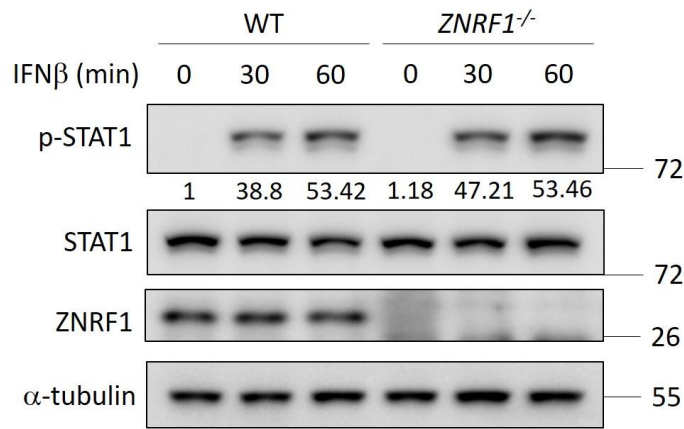
Figure 7. *ZNRf1* deficiency in CAL-1 cells enhances STAT1 activation and the expression of interferon-stimulated genes *CXCL10* and *OAS1* after stimulation with R848. WT and *ZNRf1*^{-/-} CAL-1 cells were stimulated with 1 μ g/ml R848 for the indicated times. (A) Cell lysates were collected and subjected to immunoblotted with the indicated antibodies. The intensity of p-STAT1 signal is expressed as fold induction compared to the untreated wild type cells after normalized to their unphosphorylated forms. The data are representative of three independent experiments. (B) Cells were collected and the mRNA expression of *CXCL10* and *OAS1* were analyzed by RT-qPCR.

* $P < 0.05$, ** $P < 0.01$, *** $P < 0.001$ (Student's *t*-test). The data are representative of three independent experiments performed in triplicate (error bars, s.d.).





(A)



(B)

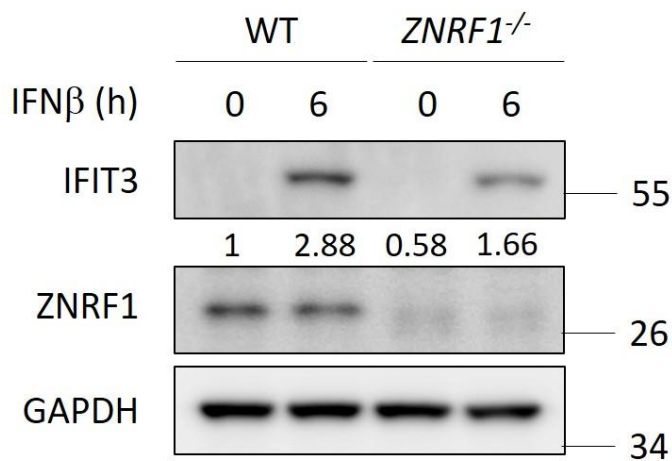


Figure 8. ZNRFI is not involved in the type I IFN signaling pathway. (A and B) WT

and *ZNRFI*^{-/-} CAL-1 cells were stimulated with IFN β for the indicated times. Cell lysates were collected and subjected to immunoblotting with the indicated antibodies.

(A) The intensity of p-STAT1 signal is expressed as fold induction compared to the untreated wild type cells after normalized to their unphosphorylated forms. The data are representative of two independent experiments. (B) The intensity of IFIT3 signal is

expressed as fold induction compared to the untreated wild type cells after normalized to the internal control GAPDH. The data was performed only once.



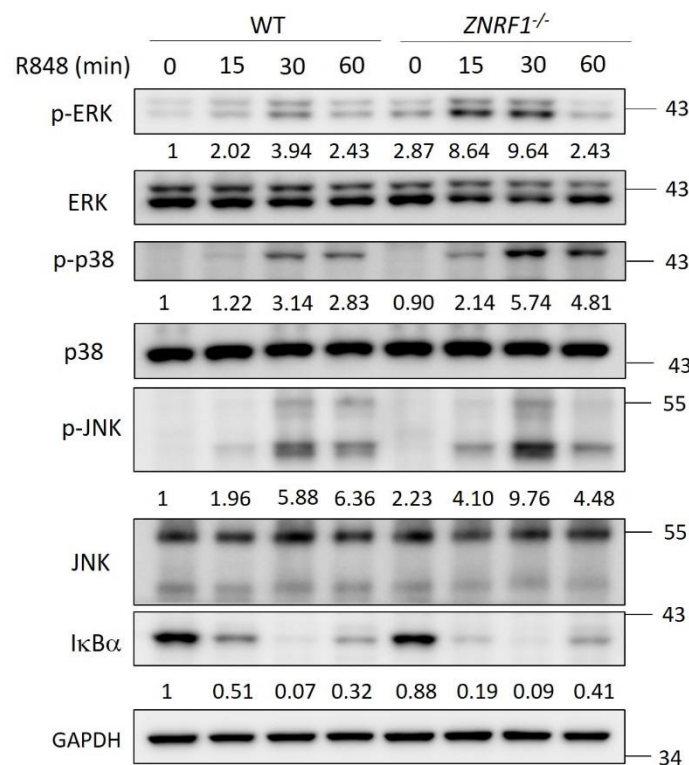
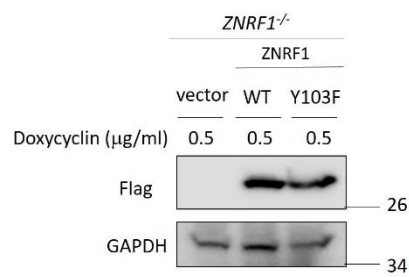


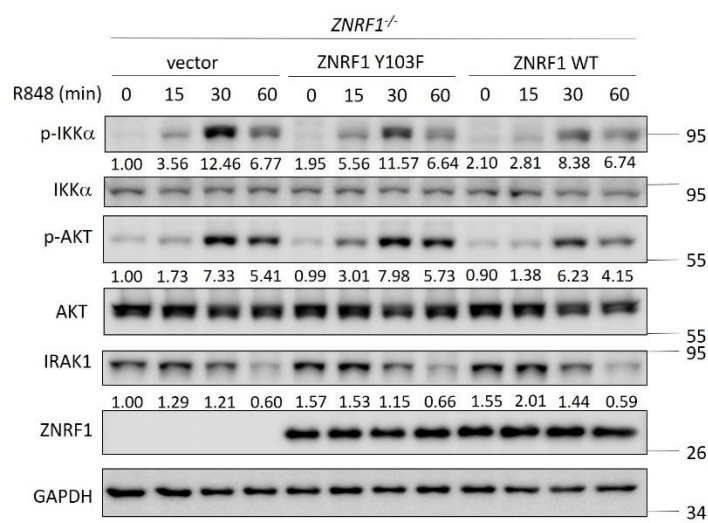
Figure 9. ZNRF1 deficiency enhances MAPK activation in CAL-1 cells after stimulation with R848. WT and *ZNRF1*^{-/-} CAL-1 cells were stimulated with 1 µg/ml R848 for the indicated times. Cell lysates were collected and immunoblotted with the indicated antibodies. The intensities of p-p38, p-JNK and p-ERK signals are expressed as fold induction compared to the untreated wild type cells after normalized to their unphosphorylated forms. The intensity of IκBα signal is expressed as fold induction compared to the untreated wild type cells after normalized to the internal control GAPDH. The data are representative of four independent experiments.



(A)



(B)



(C)

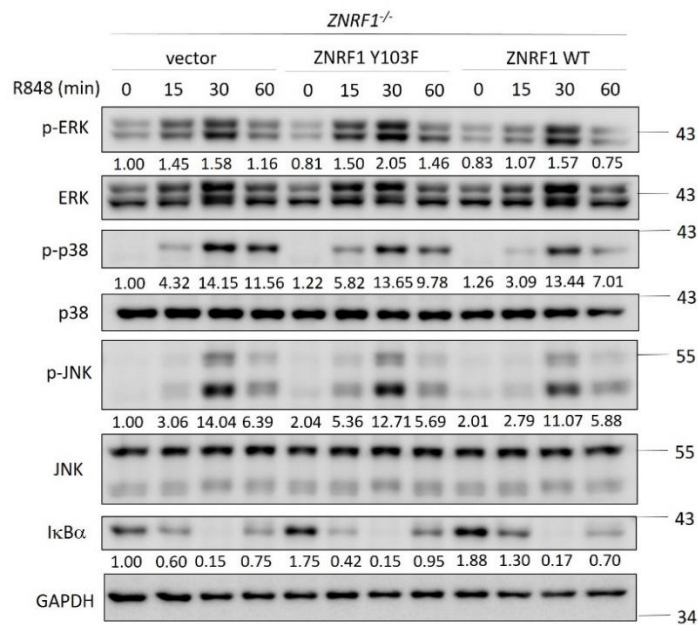


Figure 10. ZNRF1 Y103 is critical for TLR7-induced IKK α , MAPKs and

IKK β /NF- κ B activation. *ZNRF1*^{-/-} CAL-1 cells were reconstituted with inducible

vector, Flagged-tagged WT ZNRF1 or ZNRF1 (Y103F) mutant. ZNRF1 protein

expression was induced by 0.5 μ g/ml doxycycline 24 h prior to the experiment. (A) Cell

lysates of *ZNRF1*^{-/-} CAL-1 cells reconstituted with vector, ZNRF1 WT and ZNRF1

(Y103F) were collected and analyzed by immunoblotting with the indicated antibodies.

(B and C) *ZNRF1*^{-/-} CAL-1 cells reconstituted with vector, WT ZNRF1 or ZNRF1

(Y103F) were stimulated with 1 μ g/ml R848 for the indicated times. Cell lysates were

collected and analyzed by immunoblotting with the indicated antibodies. The intensities

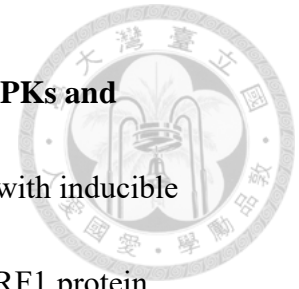
of phospho-protein signals are expressed as fold induction compared to those of

untreated vector control cells after normalized to their unphosphorylated forms. The

intensities of IRAK1 and I κ B α bands are expressed as fold induction compared to those

of untreated vector control cells after normalized to the internal control GAPDH. The

data are representative of two independent experiments.



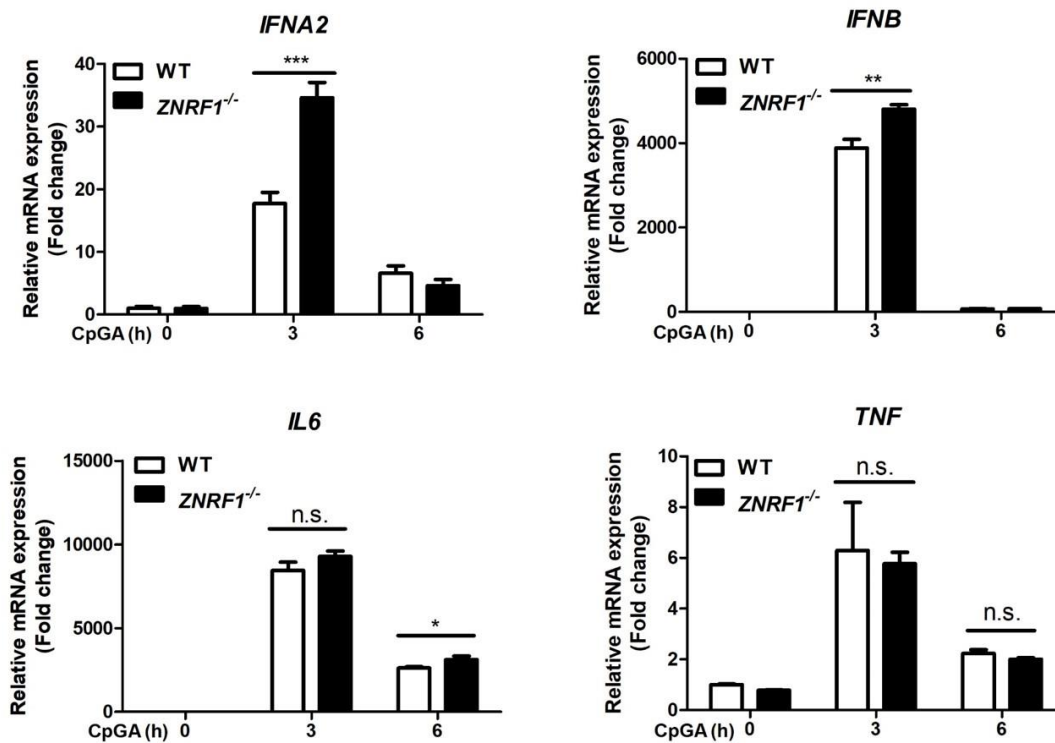


Figure 11. *ZNRFF1* depletion induced TLR9-driven type I IFNs but not pro-inflammatory cytokines production in CAL-1 cells. WT and *ZNRFF1*^{-/-} CAL-1 cells were stimulated with 3 μM CpGA for the indicated times. The mRNA expression of indicated genes were analyzed by RT-qPCR. *P<0.05, **P<0.01, ***P<0.001 (Student's *t*-test). The data are representative of three independent experiments performed in triplicate (error bars, s.d.).

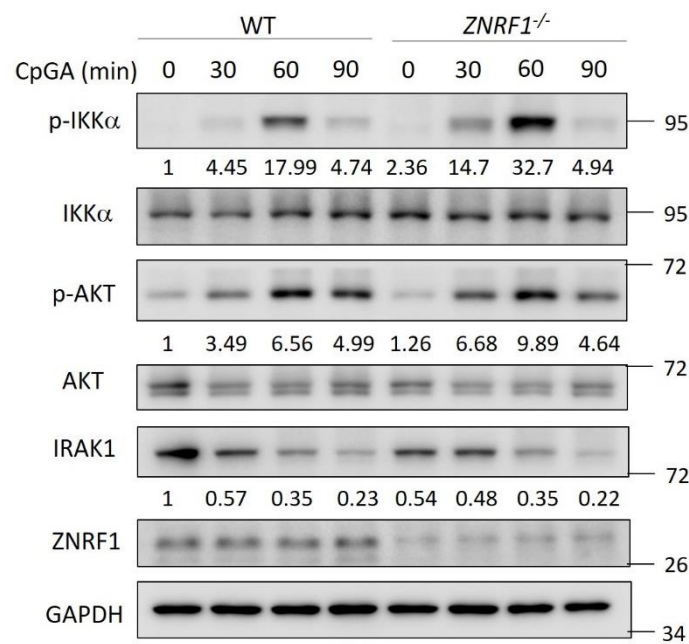


Figure 12. ZNRF1 deficiency promotes IKKα activation in CAL-1 cells after TLR9

activation. WT and *ZNRF1*^{-/-} CAL-1 cells were stimulated with 3 μM CpGA for the indicated times. Cell lysates were collected and immunoblotted with the indicated antibodies. The intensities of p-IKKα and p-AKT signals are expressed as fold induction compared to the untreated wild type cells after normalized to their unphosphorylated forms. The intensity of IRAK1 signal is expressed as fold induction compared to the untreated wild type cells after normalized to the internal control GAPDH. The data are representative of three independent experiments.

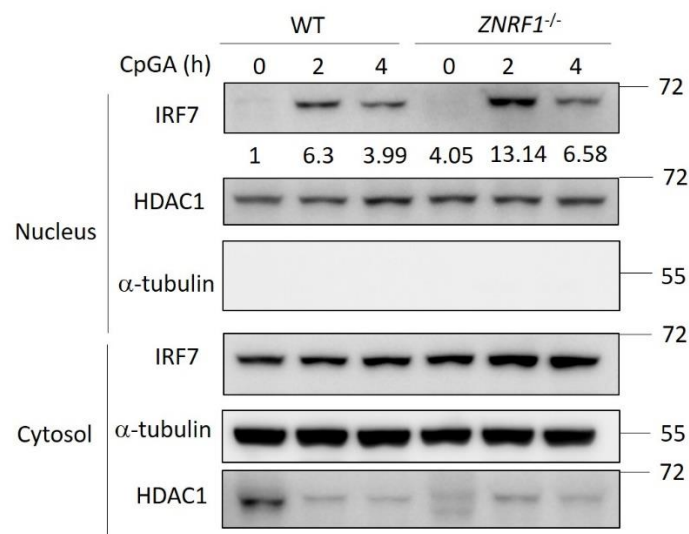
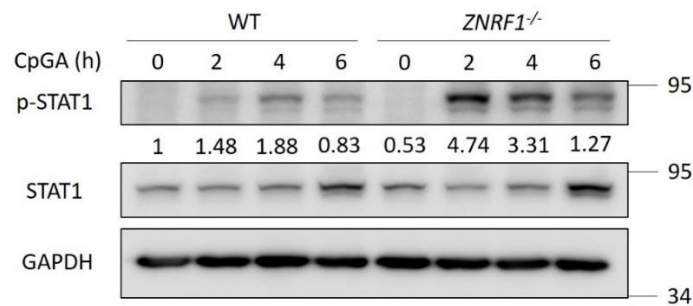


Figure 13. ZNR1 deficiency enhances IRF7 activation in CAL-1 cells after stimulation with CpGA. WT and *ZNR1*^{-/-} CAL-1 cells were stimulated with 3 μM CpGA for the indicated times. Cells were collected and subjected to the subcellular fractionation to obtain the cytosolic and nuclear fractions followed by immunoblotted with the indicated antibodies. HDAC1 and α-tubulin serve as the markers for the nuclear and cytosolic fractions, respectively. The data are representative of two independent experiments.



(A)



(B)

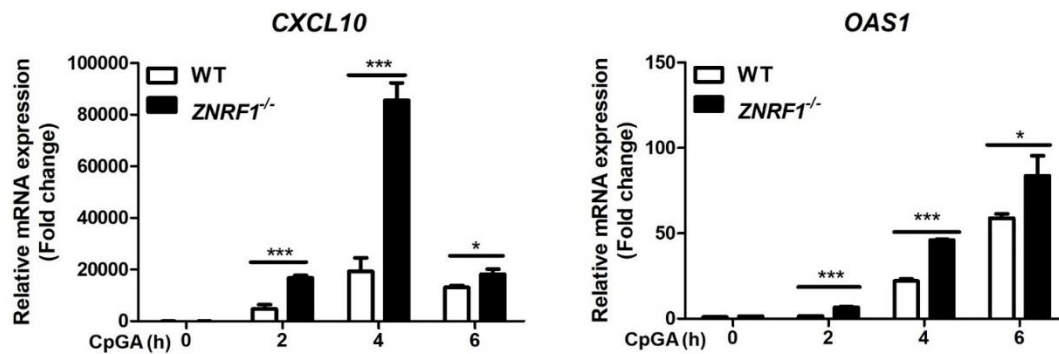


Figure 14. ZNR1 deficiency in CAL-1 cells enhances STAT1 activation and the expression of interferon-stimulated genes *CXCL10* and *OAS1* upon TLR9

activation. WT and ZNR1^{-/-} CAL-1 cells were stimulated with 3 μ M CpGA for the indicated times. (A) Cell lysates were collected and immunoblotted with the indicated antibodies. The intensity of p-STAT1 signal is expressed as fold induction compared to the untreated wild type cells after normalized to their unphosphorylated forms. The data are representative of three independent experiments. (B) Cells were collected and the mRNA expression of *CXCL10* and *OAS1* were quantified by RT-qPCR. *P<0.05, **P<0.01, ***P<0.001 (Student's *t*-test) The data are representative of three

independent experiments performed in triplicate (error bars, s.d.).



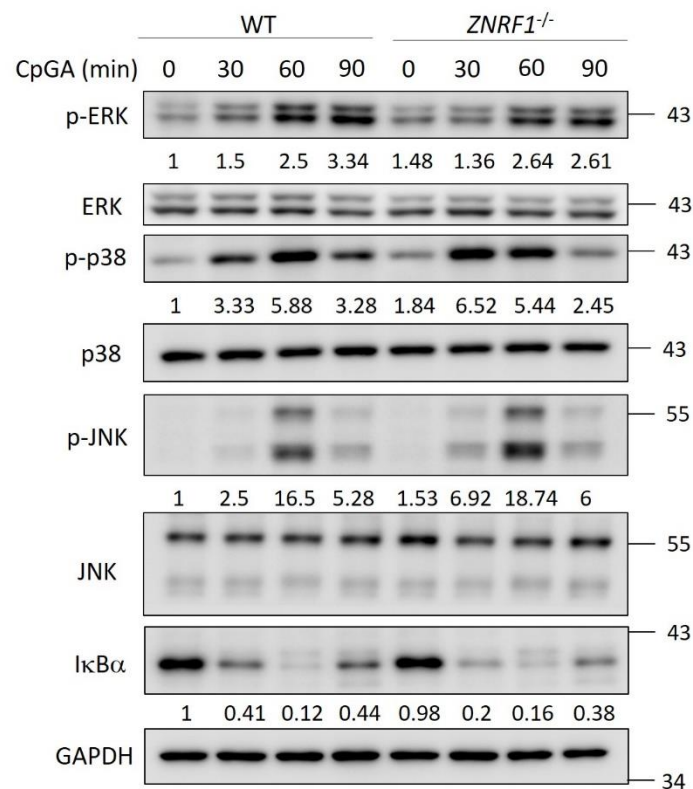
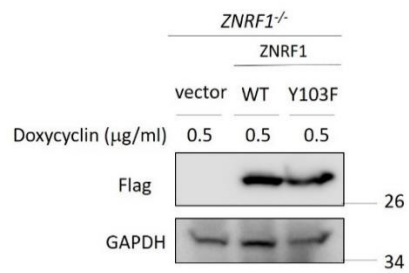


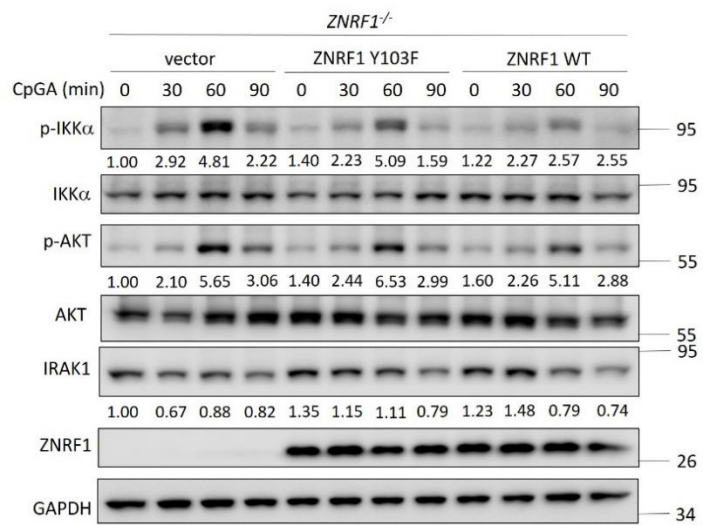
Figure 15. *ZNRFI* deficiency in CAL-1 cells has little impact on MAPK activation after stimulation with CpGA. WT and *ZNRFI*^{-/-} CAL-1 cells were stimulated with 3 μM CpGA for the indicated times. Cell lysates were collected and immunoblotted with the indicated antibodies. The intensities of p-p38, p-JNK and p-ERK signals are expressed as fold induction compared to the untreated wild type cells after normalized to their unphosphorylated forms. The intensity of IκBα signal is expressed as fold induction compared to the untreated wild type cells after normalized to the internal control GAPDH. The data are representative of three independent experiments.



(A)



(B)



(C)

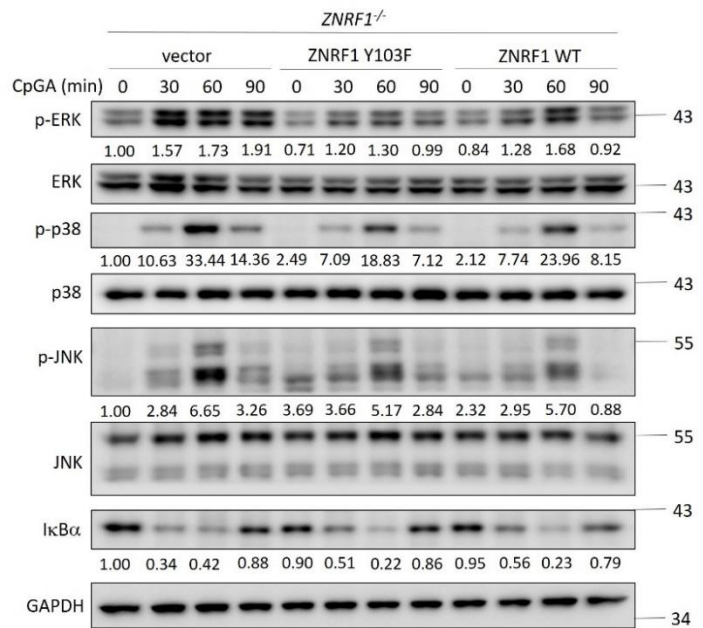



Figure 16. Y103 of ZNRF1 is critical for TLR9-induced IKK α and AKT activation.



ZNRF1^{-/-} CAL-1 cells were reconstituted with inducible vector, Flagged-tagged WT ZNRF1 or ZNRF1 (Y103F) mutant. ZNRF1 protein expression was induced by 0.5 μ g/ml doxycycline 24 h prior to the experiment. (A) Cell lysates of *ZNRF1*^{-/-} CAL-1 cells reconstituted with vector, WT ZNRF1 and ZNRF1 (Y103F) mutant were collected and subjected to immunoblotting with the indicated antibodies. (B and C) *ZNRF1*^{-/-} CAL-1 cells reconstituted with vector, WT ZNRF1 and ZNRF1 (Y103F) mutant were stimulated with 1 μ g/ml R848 for the indicated times. Cell lysates were collected and subjected to immunoblotting with the indicated antibodies. The intensities of phospho-protein signals are expressed as fold induction compared to those of untreated vector control cells after normalized to their unphosphorylated forms. The intensities of IRAK1 and I κ B α signals are expressed as fold induction compared to those of untreated vector control cells after normalized to the internal control GAPDH.

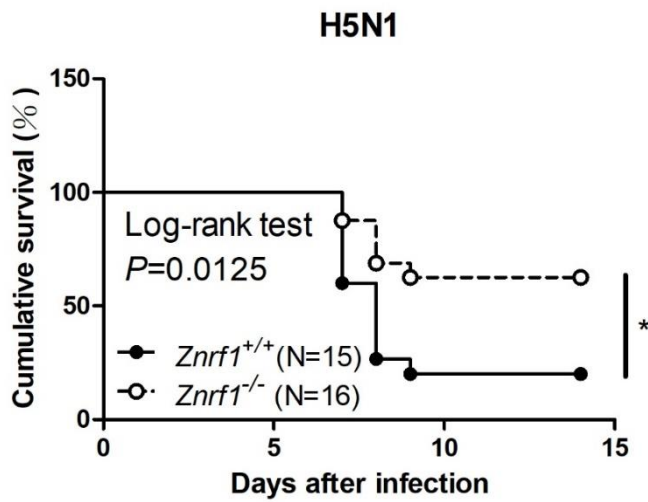
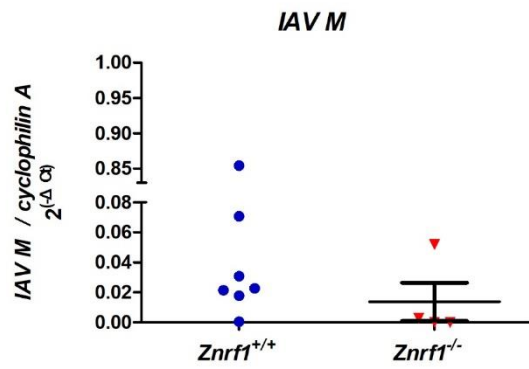


Figure 17. $Znrfl^{-/-}$ mice are more resistant to H5N1 influenza virus infection.

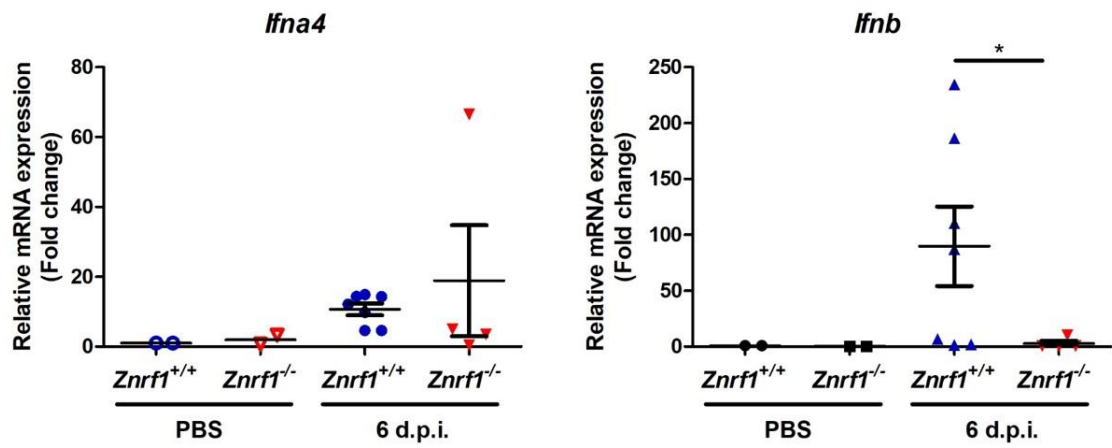
$Znrfl^{+/+}$ mice and $Znrfl^{-/-}$ mice were infected with 1500 PFU of influenza A virus H5N1 by intratrachea (i.t.) injection. The survival of infected mice was monitored for 14 days after infection. $Znrfl^{+/+}$, n=15 and $Znrfl^{-/-}$, n=16. Data are pooled from four independent experiments, and analyzed by the log-rank test. * $P<0.05$



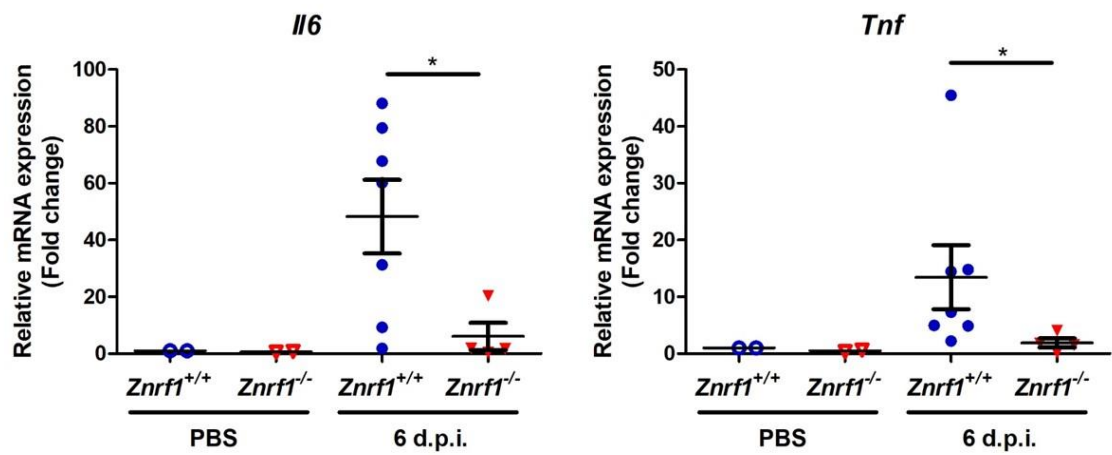
(A)

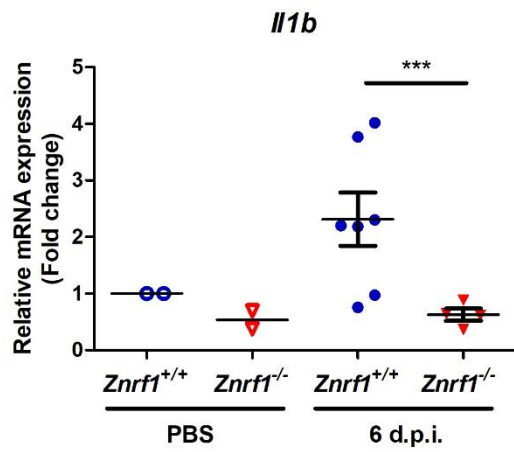


(B)

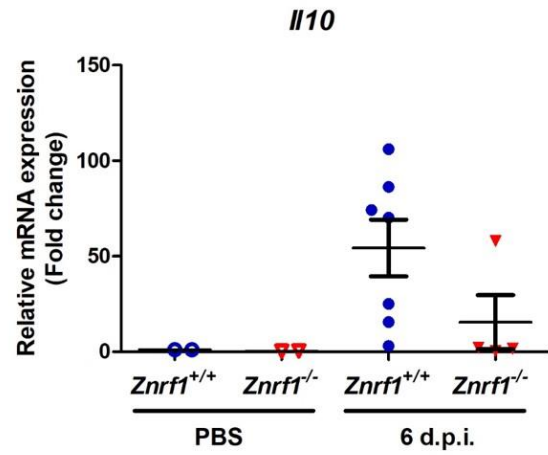
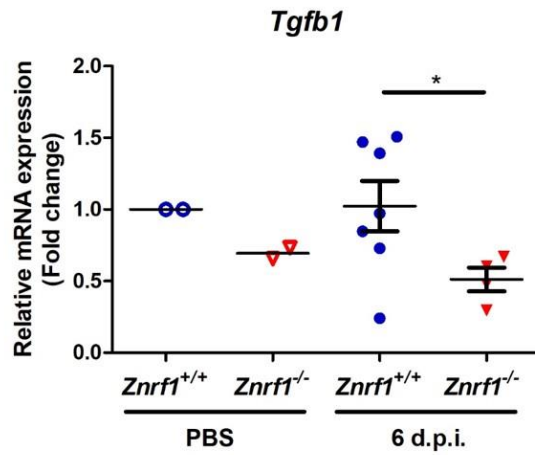


(C)

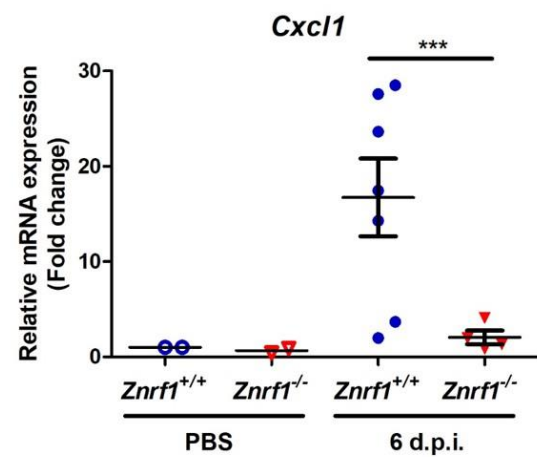
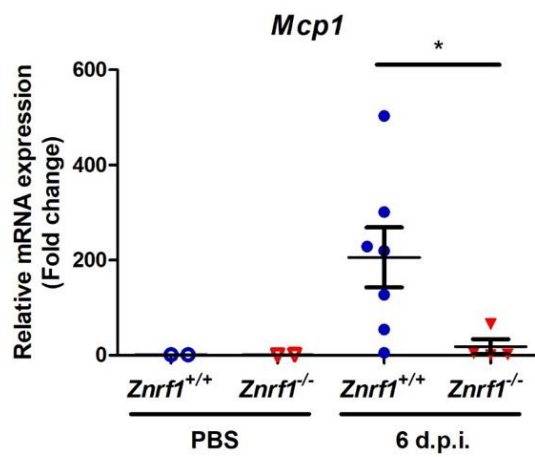




(D)



(E)



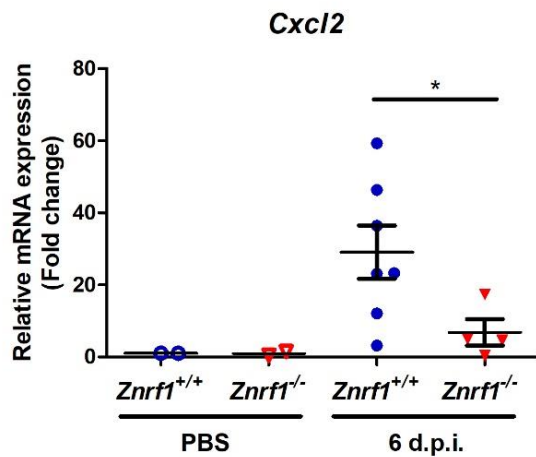
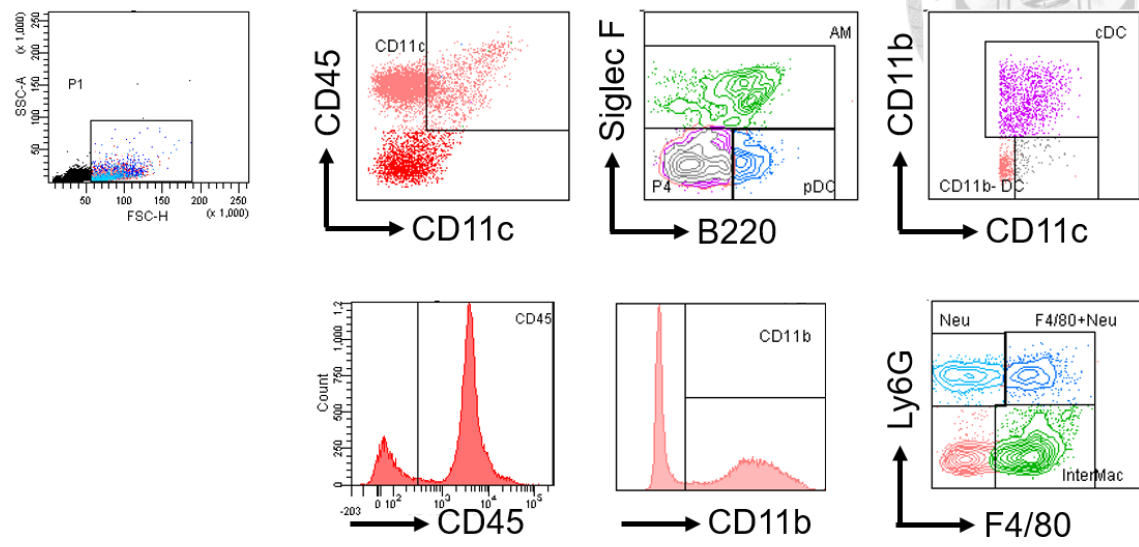
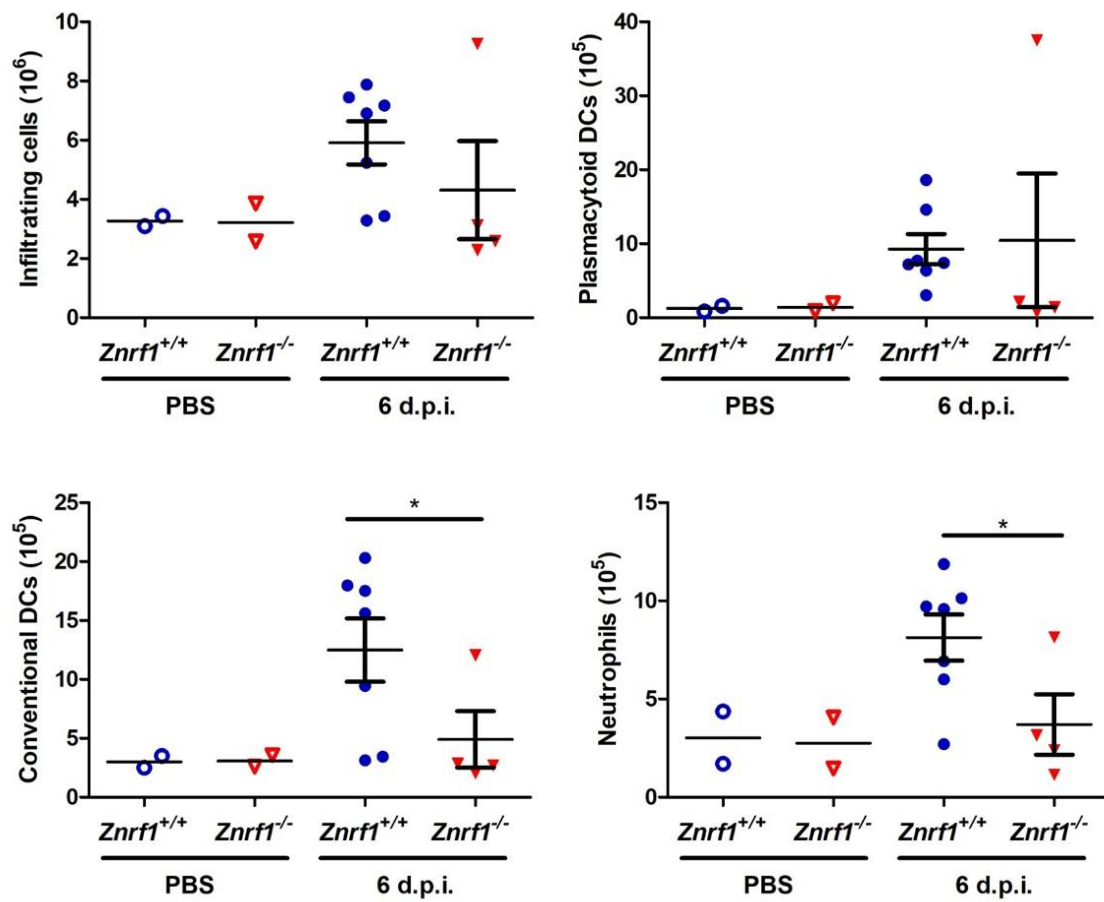


Figure 18. *Znrfl*^{-/-} mice displayed reduced levels of pro-inflammatory cytokines and chemokines after H5N1 influenza virus infection. *Znrfl*^{+/+} mice and *Znrfl*^{-/-} mice were injected with PBS or infected with H5N1 virus (1500 pfu) by intratrachea injection. At day 6 of viral infection, lungs from naïve and infected mice were harvested and subject to RNA extraction. The mRNA levels of IAV M and the indicated genes in lung samples were analyzed by RT-qPCR. Relative fold induction of the mRNAs were normalized to that in the naïve *Znrfl*^{+/+} group. *P<0.05, **P<0.01, ***P<0.001 (Student's *t*-test). Each symbol represents an individual mouse.

(A)



(B)



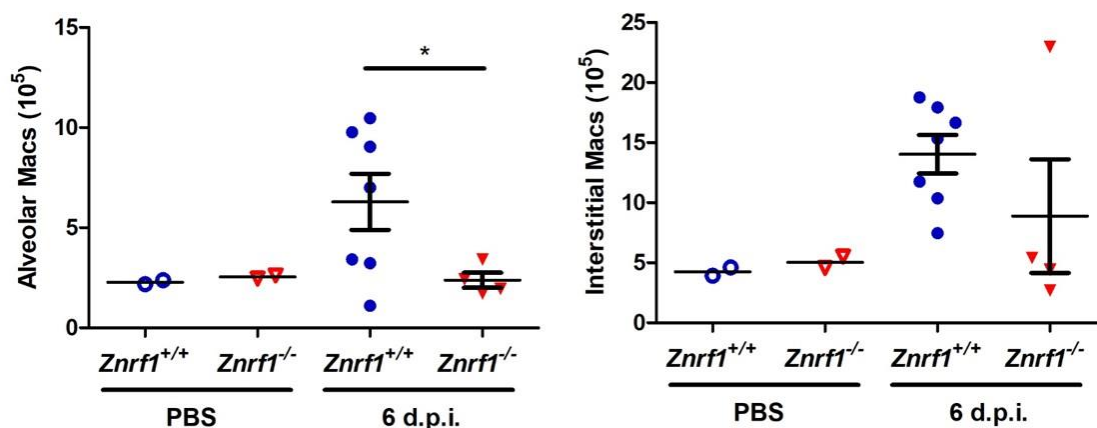


Figure 19. *Znrfl*^{-/-} mice showed reduced numbers of alveolar macrophages, conventional DCs and neutrophils in lungs after influenza virus H5N1 infection.

Znrfl^{+/+} mice and *Znrfl*^{-/-} mice were intratracheally injected with PBS or H5N1 virus (1500 pfu). At day 6 of infection, mouse lungs were harvested and digested by Liberase TM followed by flow cytometry analysis of immune cell populations. (A) Flow cytometry gating strategy for analysis of lung immune cell populations: all leukocytes cells (CD45⁺), plasmacytoid dendritic cells (CD45⁺CD11C⁺B220⁺), conventional dendritic cells (CD45⁺CD11C⁺CD11b⁺SiglecF⁻B220⁻), neutrophils (CD45⁺CD11b⁺Ly6G⁺), alveolar macrophages (CD45⁺CD11c⁺SiglecF⁺), and interstitial macrophages (CD45⁺CD11b⁺F4/80⁺). (B) Total number changes of lung immune cell populations in *Znrfl*^{+/+} and *Znrfl*^{-/-} mice challenged with PBS or H5N1 IAV. Data are pooled from two independent experiments. *P<0.05, **P<0.01, ***P<0.001 (Student's *t*-test)

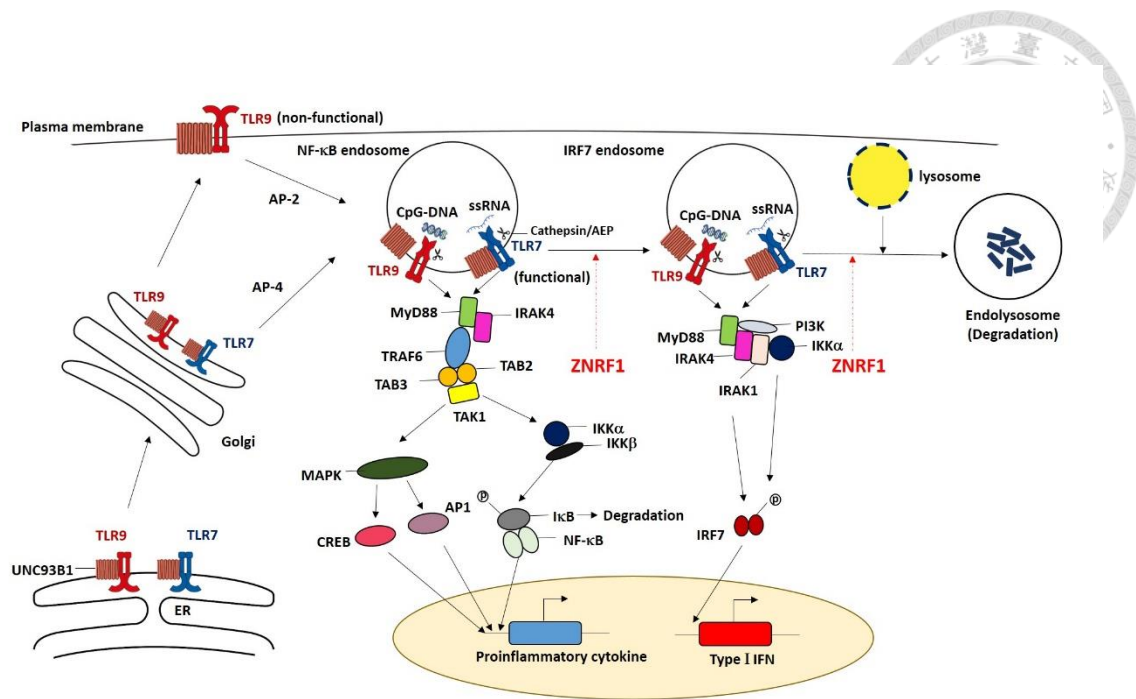
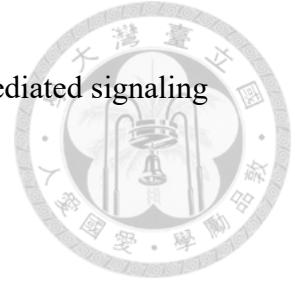


Figure 20. The proposed model for the regulation of TLR7 and TLR9-mediated immune response by ZNRF1 in pDCs. Upon stimulation with ligands, TLR7 directly traffics to the endosomes by recruiting the AP-4 complex, a sorting complex, whereas TLR9 transports to the plasma membrane followed by translocating to the endosomes via AP-2-mediated endocytosis. TLR7 and TLR9 encountered their ligands at the early endosomes, where they induce the transcription of pro-inflammatory genes via activation of NF-κB. Later, TLR7 and TLR9 together with their ligands are transported to the lysosome-related organelles (LROs), also called IRF7 endosome, and turn on type I IFNs production. In this study, ZNRF1 is suggested to limit the activity of IKKα, which prevents IRF7 hyperactivation, overproduction of type I IFNs and ISGs. Moreover, ZNRF1 is not involved in the type I IFN pathway. Thus, we hypothesize that ZNRF1 might control TLR7 and TLR9 transporting to the lysosomes for degradation. In

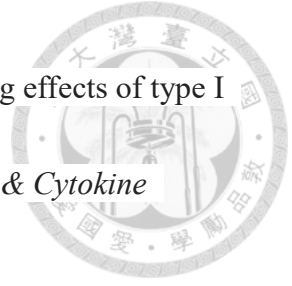
addition, Y103 residue of ZNRF1 is critical for TLR7- and TLR9-mediated signaling pathway.



References



1. Takeuchi, O., & Akira, S. (2010). Pattern recognition receptors and inflammation. *Cell*, 140(6), 805-820.
2. Akira, S., Uematsu, S., & Takeuchi, O. (2006). Pathogen recognition and innate immunity. *Cell*, 124(4), 783-801.
3. Beutler, B., Jiang, Z., Georgel, P., Crozat, K., Croker, B., Rutschmann, S., ... & Hoebe, K. (2006). Genetic analysis of host resistance: Toll-like receptor signaling and immunity at large. *Annu. Rev. Immunol.*, 24, 353-389.
4. Tang, D., Kang, R., Coyne, C. B., Zeh, H. J., & Lotze, M. T. (2012). PAMP s and DAMP s: signal 0s that spur autophagy and immunity. *Immunological reviews*, 249(1), 158-175.
5. Brubaker, S. W., Bonham, K. S., Zanoni, I., & Kagan, J. C. (2015). Innate immune pattern recognition: a cell biological perspective. *Annual review of immunology*, 33, 257-290.
6. Basit, A., Cho, M. G., Kim, E. Y., Kwon, D., Kang, S. J., & Lee, J. H. (2020). The cGAS/STING/TBK1/IRF3 innate immunity pathway maintains chromosomal stability through regulation of p21 levels. *Experimental & Molecular Medicine*, 52(4), 643-657.
7. Mogensen, T. H. (2009). Pathogen recognition and inflammatory signaling in innate immune defenses. *Clinical microbiology reviews*, 22(2), 240-273.



8. Davidson, S., Maini, M. K., & Wack, A. (2015). Disease-promoting effects of type I interferons in viral, bacterial, and coinfections. *Journal of Interferon & Cytokine Research*, 35(4), 252-264.
9. Carpenter, S., Ricci, E. P., Mercier, B. C., Moore, M. J., & Fitzgerald, K. A. (2014). Post-transcriptional regulation of gene expression in innate immunity. *Nature Reviews Immunology*, 14(6), 361-376.
10. Deretic, V., Saitoh, T., & Akira, S. (2013). Autophagy in infection, inflammation and immunity. *Nature Reviews Immunology*, 13(10), 722-737.
11. Cao, X. (2016). Self-regulation and cross-regulation of pattern-recognition receptor signalling in health and disease. *Nature Reviews Immunology*, 16(1), 35.
12. Anderson, K. V., Jürgens, G., & Nüsslein-Volhard, C. (1985). Establishment of dorsal-ventral polarity in the *Drosophila* embryo: genetic studies on the role of the Toll gene product. *Cell*, 42(3), 779-789.
13. Lemaitre, B., Nicolas, E., Michaut, L., Reichhart, J. M., & Hoffmann, J. A. (1996). The dorsoventral regulatory gene cassette *spätzle*/Toll/cactus controls the potent antifungal response in *Drosophila* adults. *Cell*, 86(6), 973-983.
14. Kawasaki, T., & Kawai, T. (2014). Toll-like receptor signaling pathways. *Frontiers in immunology*, 5, 461.
15. Kawai, T., & Akira, S. (2010). The role of pattern-recognition receptors in innate

immunity: update on Toll-like receptors. *Nature immunology*, 11(5), 373.

16. Celhar, T., Magalhaes, R., & Fairhurst, A. M. (2012). TLR7 and TLR9 in SLE:

when sensing self goes wrong. *Immunologic research*, 53(1-3), 58-77.

17. O'Neill, L. A., Golenbock, D., & Bowie, A. G. (2013). The history of Toll-like

receptors—redefining innate immunity. *Nature Reviews Immunology*, 13(6), 453-460.

18. Majer, O., Liu, B., & Barton, G. M. (2017). Nucleic acid-sensing TLRs: trafficking

and regulation. *Current opinion in immunology*, 44, 26-33.

19. He, X., Jia, H., Jing, Z., & Liu, D. (2013). Recognition of pathogen-associated

nucleic acids by endosomal nucleic acid-sensing toll-like receptors. *Acta Biochim*

Biophys Sin, 45(4), 241-258.

20. Roers, A., Hiller, B., & Hornung, V. (2016). Recognition of endogenous nucleic

acids by the innate immune system. *Immunity*, 44(4), 739-754.

21. Oldenburg, M., Krüger, A., Ferstl, R., Kaufmann, A., Nees, G., Sigmund, A., ... &

Koedel, U. (2012). TLR13 recognizes bacterial 23S rRNA devoid of erythromycin

resistance-forming modification. *Science*, 337(6098), 1111-1115.

22. Lester, S. N., & Li, K. (2014). Toll-like receptors in antiviral innate

immunity. *Journal of molecular biology*, 426(6), 1246-1264.

23. Diebold, S. S., Kaisho, T., Hemmi, H., Akira, S., & e Sousa, C. R. (2004). Innate

antiviral responses by means of TLR7-mediated recognition of single-stranded



RNA. *Science*, 303(5663), 1529-1531.

24. Solmaz, G., Puttur, F., Francozo, M., Lindenberg, M., Guderian, M., Swallow, M., ... & Clausen, B. E. (2019). TLR7 Controls VSV Replication in CD169+ SCS

Macrophages and Associated Viral Neuroinvasion. *Frontiers in immunology*, 10, 466.

25. Heil, F., Hemmi, H., Hochrein, H., Ampenberger, F., Kirschning, C., Akira, S., ... & Bauer, S. (2004). Species-specific recognition of single-stranded RNA via toll-like receptor 7 and 8. *Science*, 303(5663), 1526-1529.

26. Melchjorsen, J., Jensen, S. B., Malmgaard, L., Rasmussen, S. B., Weber, F., Bowie, A. G., ... & Paludan, S. R. (2005). Activation of innate defense against a paramyxovirus is mediated by RIG-I and TLR7 and TLR8 in a cell-type-specific manner. *Journal of virology*, 79(20), 12944-12951.

27. Takahashi, K., Asabe, S., Wieland, S., Garaigorta, U., Gastaminza, P., Isogawa, M., & Chisari, F. V. (2010). Plasmacytoid dendritic cells sense hepatitis C virus–infected cells, produce interferon, and inhibit infection. *Proceedings of the National Academy of Sciences*, 107(16), 7431-7436.

28. Cervantes-Barragan, L., Züst, R., Weber, F., Spiegel, M., Lang, K. S., Akira, S., ... & Ludewig, B. (2007). Control of coronavirus infection through plasmacytoid dendritic-cell–derived type I interferon. *Blood*, 109(3), 1131-1137.

29. Tabeta, K., Georgel, P., Janssen, E., Du, X., Hoebe, K., Crozat, K., ... &



Alexopoulou, L. (2004). Toll-like receptors 9 and 3 as essential components of innate immune defense against mouse cytomegalovirus infection. *Proceedings of the National Academy of Sciences*, 101(10), 3516-3521.

30. Krug, A., Luker, G. D., Barchet, W., Leib, D. A., Akira, S., & Colonna, M. (2004).

Herpes simplex virus type 1 activates murine natural interferon-producing cells through toll-like receptor 9. *Blood*, 103(4), 1433-1437.


31. Lund, J., Sato, A., Akira, S., Medzhitov, R., & Iwasaki, A. (2003). Toll-like receptor 9-mediated recognition of Herpes simplex virus-2 by plasmacytoid dendritic cells. *The Journal of experimental medicine*, 198(3), 513-520.

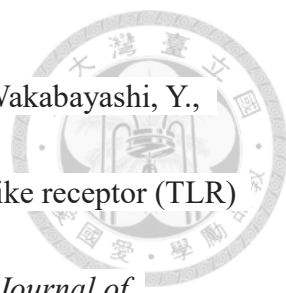
32. Samuelsson, C., Hausmann, J., Lauterbach, H., Schmidt, M., Akira, S., Wagner, H., ... & Hochrein, H. (2008). Survival of lethal poxvirus infection in mice depends on TLR9, and therapeutic vaccination provides protection. *The Journal of clinical investigation*, 118(5), 1776-1784.

33. Reizis, B. (2019). Plasmacytoid dendritic cells: development, regulation, and function. *Immunity*, 50(1), 37-50.

34. Fitzgerald-Bocarsly, P., & Feng, D. (2007). The role of type I interferon production by dendritic cells in host defense. *Biochimie*, 89(6-7), 843-855.

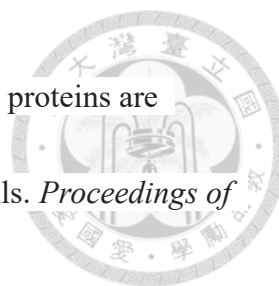
35. McKenna, K., Beignon, A. S., & Bhardwaj, N. (2005). Plasmacytoid dendritic cells: linking innate and adaptive immunity. *Journal of virology*, 79(1), 17-27.

- 
36. Vidya, M. K., Kumar, V. G., Sejian, V., Bagath, M., Krishnan, G., & Bhatta, R. (2018). Toll-like receptors: significance, ligands, signaling pathways, and functions in mammals. *International Reviews of Immunology*, 37(1), 20-36.
37. Delhase, M., Hayakawa, M., Chen, Y., & Karin, M. (1999). Positive and negative regulation of I κ B kinase activity through IKK β subunit phosphorylation. *Science*, 284(5412), 309-313.
38. Gilliet, M., Cao, W., & Liu, Y. J. (2008). Plasmacytoid dendritic cells: sensing nucleic acids in viral infection and autoimmune diseases. *Nature Reviews Immunology*, 8(8), 594-606.
39. Saleiro, D., Mehrotra, S., Kroczyńska, B., Beauchamp, E. M., Lisowski, P., Majchrzak-Kita, B., ... & Kosciuczuk, E. M. (2015). Central role of ULK1 in type I interferon signaling. *Cell reports*, 11(4), 605-617.
40. Platanias, L. C. (2005). Mechanisms of type-I-and type-II-interferon-mediated signalling. *Nature Reviews Immunology*, 5(5), 375-386.
41. Van Pesch, V., Lanaya, H., Renauld, J. C., & Michiels, T. (2004). Characterization of the murine alpha interferon gene family. *Journal of virology*, 78(15), 8219-8228.
42. Yang, Y., Liu, B., Dai, J., Srivastava, P. K., Zammit, D. J., Lefrançois, L., & Li, Z. (2007). Heat shock protein gp96 is a master chaperone for toll-like receptors and is important in the innate function of macrophages. *Immunity*, 26(2), 215-226.

- 
43. Takahashi, K., Shibata, T., Akashi-Takamura, S., Kiyokawa, T., Wakabayashi, Y., Tanimura, N., ... & Nagai, Y. (2007). A protein associated with Toll-like receptor (TLR) 4 (PRAT4A) is required for TLR-dependent immune responses. *The Journal of experimental medicine*, 204(12), 2963-2976.
44. Kim, Y. M., Brinkmann, M. M., Paquet, M. E., & Ploegh, H. L. (2008). UNC93B1 delivers nucleotide-sensing toll-like receptors to endolysosomes. *Nature*, 452(7184), 234-238.
45. Pelka, K., Bertheloot, D., Reimer, E., Phulphagar, K., Schmidt, S. V., Christ, A., ... & Haas, A. (2018). The chaperone UNC93B1 regulates Toll-like receptor stability independently of endosomal TLR transport. *Immunity*, 48(5), 911-922.
46. Fukui, R., Saitoh, S. I., Kanno, A., Onji, M., Shibata, T., Ito, A., ... & Miyake, K. (2011). Unc93B1 restricts systemic lethal inflammation by orchestrating Toll-like receptor 7 and 9 trafficking. *Immunity*, 35(1), 69-81.
47. Majer, O., Liu, B., Woo, B. J., Kreuk, L. S., Van Dis, E., & Barton, G. M. (2019). Release from UNC93B1 reinforces the compartmentalized activation of select TLRs. *Nature*, 575(7782), 371-374.
48. Majer, O., Liu, B., Kreuk, L. S., Krogan, N., & Barton, G. M. (2019). UNC93B1 recruits syntenin-1 to dampen TLR7 signalling and prevent autoimmunity. *Nature*, 575(7782), 366-370.



49. Lee, B. L., & Barton, G. M. (2014). Trafficking of endosomal Toll-like receptors. *Trends in cell biology*, 24(6), 360-369.
50. Tatematsu, M., Funami, K., Ishii, N., Seya, T., Obuse, C., & Matsumoto, M. (2015). LRRC59 regulates trafficking of nucleic acid-sensing TLRs from the endoplasmic reticulum via association with UNC93B1. *The Journal of Immunology*, 195(10), 4933-4942.
51. Chiang, C. Y., Engel, A., Opaluch, A. M., Ramos, I., Maestre, A. M., Secundino, I., ... & Miraglia, L. J. (2012). Cofactors required for TLR7-and TLR9-dependent innate immune responses. *Cell host & microbe*, 11(3), 306-318.
52. Honda, K., Ohba, Y., Yanai, H., Negishi, H., Mizutani, T., Takaoka, A., ... & Taniguchi, T. (2005). Spatiotemporal regulation of MyD88-IRF-7 signalling for robust type-I interferon induction. *Nature*, 434(7036), 1035-1040.
53. Guiducci, C., Ott, G., Chan, J. H., Damon, E., Calacsan, C., Matray, T., ... & Barrat, F. J. (2006). Properties regulating the nature of the plasmacytoid dendritic cell response to Toll-like receptor 9 activation. *The Journal of experimental medicine*, 203(8), 1999-2008.
54. Sasai, M., Linchan, M. M., & Iwasaki, A. (2010). Bifurcation of Toll-like receptor 9 signaling by adaptor protein 3. *Science*, 329(5998), 1530-1534.
55. Blasius, A. L., Arnold, C. N., Georgel, P., Rutschmann, S., Xia, Y., Lin, P., ... &



Beutler, B. (2010). Slc15a4, AP-3, and Hermansky-Pudlak syndrome proteins are required for Toll-like receptor signaling in plasmacytoid dendritic cells. *Proceedings of the National Academy of Sciences*, 107(46), 19973-19978.

56. Henault, J., Martinez, J., Riggs, J. M., Tian, J., Mehta, P., Clarke, L., ... & Coyle, A.

J. (2012). Noncanonical autophagy is required for type I interferon secretion in response to DNA-immune complexes. *Immunity*, 37(6), 986-997.

57. Ewald, S. E., Lee, B. L., Lau, L., Wickliffe, K. E., Shi, G. P., Chapman, H. A., &

Barton, G. M. (2008). The ectodomain of Toll-like receptor 9 is cleaved to generate a functional receptor. *Nature*, 456(7222), 658-662.

58. Barton, G. M., Kagan, J. C., & Medzhitov, R. (2006). Intracellular localization of

Toll-like receptor 9 prevents recognition of self DNA but facilitates access to viral DNA. *Nature immunology*, 7(1), 49-56.

59. Ewald, S. E., Engel, A., Lee, J., Wang, M., Bogyo, M., & Barton, G. M. (2011).

Nucleic acid recognition by Toll-like receptors is coupled to stepwise processing by cathepsins and asparagine endopeptidase. *Journal of Experimental Medicine*, 208(4), 643-651.

60. Kanno, A., Yamamoto, C., Onji, M., Fukui, R., Saitoh, S. I., Motoi, Y., ... & Miyake,

K. (2013). Essential role for Toll-like receptor 7 (TLR7)-unique cysteines in an intramolecular disulfide bond, proteolytic cleavage and RNA sensing. *International*

immunology, 25(7), 413-422.



61. Onji, M., Kanno, A., Saitoh, S. I., Fukui, R., Motoi, Y., Shibata, T., ... & Yamamoto, K. (2013). An essential role for the N-terminal fragment of Toll-like receptor 9 in DNA

sensing. *Nature communications*, 4(1), 1-10.

62. Swatek, K. N., & Komander, D. (2016). Ubiquitin modifications. *Cell*

research, 26(4), 399-422.

63. Hu, H., & Sun, S. C. (2016). Ubiquitin signaling in immune responses. *Cell*

research, 26(4), 457-483.

64. Sun, S. C. (2008). Deubiquitylation and regulation of the immune response. *Nature*

Reviews Immunology, 8(7), 501-511.

65. Manohar, S., Jacob, S., Wang, J., Wiechecki, K. A., Koh, H. W., Simões, V., ... &

Silva, G. M. (2019). Polyubiquitin chains linked by lysine residue 48 (K48) selectively target oxidized proteins in vivo. *Antioxidants & redox signaling*, 31(15), 1133-1149.


66. Erpapazoglou, Z., Walker, O., & Haguenauer-Tsapis, R. (2014). Versatile roles of

k63-linked ubiquitin chains in trafficking. *Cells*, 3(4), 1027-1088.

67. Messick, T. E., & Greenberg, R. A. (2009). The ubiquitin landscape at DNA double-strand breaks. *Journal of Cell Biology*, 187(3), 319-326.

68. Vallabhapurapu, S., & Karin, M. (2009). Regulation and function of NF- κ B

transcription factors in the immune system. *Annual review of immunology*, 27, 693-733.

- 
69. Wang, G., Gao, Y., Li, L., Jin, G., Chao, J. I., & Lin, H. K. (2012). K63-linked ubiquitination in kinase activation and cancer. *Frontiers in oncology*, 2, 5.
70. Chen, Z. J. (2012). Ubiquitination in signaling to and activation of IKK. *Immunological reviews*, 246(1), 95-106.
71. Kawai, T., Sato, S., Ishii, K. J., Coban, C., Hemmi, H., Yamamoto, M., ... & Takeuchi, O. (2004). Interferon- α induction through Toll-like receptors involves a direct interaction of IRF7 with MyD88 and TRAF6. *Nature immunology*, 5(10), 1061-1068.
72. Min, Y., Kim, M. J., Lee, S., Chun, E., & Lee, K. Y. (2018). Inhibition of TRAF6 ubiquitin-ligase activity by PRDX1 leads to inhibition of NF κ B activation and autophagy activation. *Autophagy*, 14(8), 1347-1358.
73. Chiang, C. Y., Engel, A., Opaluch, A. M., Ramos, I., Maestre, A. M., Secundino, I., ... & Miraglia, L. J. (2012). Cofactors required for TLR7-and TLR9-dependent innate immune responses. *Cell host & microbe*, 11(3), 306-318.
74. Araki, T., Nagarajan, R., & Milbrandt, J. (2001). Identification of genes induced in peripheral nerve after injury expression profiling and novel gene discovery. *Journal of Biological Chemistry*, 276(36), 34131-34141.
75. Pickart, C. M. (2001). Mechanisms underlying ubiquitination. *Annual review of biochemistry*, 70(1), 503-533.
76. Araki, T., & Milbrandt, J. (2003). ZNRF proteins constitute a family of presynaptic

E3 ubiquitin ligases. *Journal of Neuroscience*, 23(28), 9385-9394.

77. Wakatsuki, S., Saitoh, F., & Araki, T. (2011). ZNRF1 promotes Wallerian degeneration by degrading AKT to induce GSK3B-dependent CRMP2

phosphorylation. *Nature cell biology*, 13(12), 1415-1423.

78. Wakatsuki, S., Furuno, A., Ohshima, M., & Araki, T. (2015). Oxidative stress–dependent phosphorylation activates ZNRF1 to induce neuronal/axonal

degeneration. *Journal of Cell Biology*, 211(4), 881-896.

79. Shang, Z., Zhao, Y., Zhou, K., Xu, Y., & Huang, W. (2013). PAX5 alteration-associated gene-expression signatures in B-cell acute lymphoblastic

leukemia. *International journal of hematology*, 97(5), 599-603.

80. Lee, C. Y., Lai, T. Y., Tsai, M. K., Chang, Y. C., Ho, Y. H., Yu, I. S., ... & Hsu, L. C.

(2017). The ubiquitin ligase ZNRF1 promotes caveolin-1 ubiquitination and degradation to modulate inflammation. *Nature communications*, 8(1), 1-14.

81. Maeda, T., Murata, K., Fukushima, T., Sugahara, K., Tsuruda, K., Anami, M., ... &

Hasegawa, H. (2005). A novel plasmacytoid dendritic cell line, CAL-1, established from a patient with blastic natural killer cell lymphoma. *International journal of*

hematology, 81(2), 148-154.

82. Hilbert, T., Steinhagen, F., Weisheit, C., Baumgarten, G., Hoeft, A., & Klaschik, S.

(2015). Synergistic stimulation with different TLR7 ligands modulates gene expression



patterns in the human plasmacytoid dendritic cell line CAL-1. *Mediators of inflammation*, 2015.



83. Steinhagen, F., Meyer, C., Tross, D., Gursel, M., Maeda, T., Klaschik, S., &

Klinman, D. M. (2012). Activation of type I interferon-dependent genes characterizes the “core response” induced by CpG DNA. *Journal of leukocyte biology*, 92(4), 775-785.

84. Uematsu, S., Sato, S., Yamamoto, M., Hirotani, T., Kato, H., Takeshita, F., ... &

Takeuchi, O. (2005). Interleukin-1 receptor-associated kinase-1 plays an essential role for Toll-like receptor (TLR) 7-and TLR9-mediated interferon- α induction. *The Journal of experimental medicine*, 201(6), 915-923.

85. Hoshino, K., Sugiyama, T., Matsumoto, M., Tanaka, T., Saito, M., Hemmi, H., ... &

Kaisho, T. (2006). I κ B kinase- α is critical for interferon- α production induced by Toll-like receptors 7 and 9. *Nature*, 440(7086), 949-953.

86. Guiducci, C., Ghirelli, C., Marloie-Provost, M. A., Matray, T., Coffman, R. L., Liu,

Y. J., ... & Soumelis, V. (2008). PI3K is critical for the nuclear translocation of IRF-7 and type I IFN production by human plasmacytoid predendritic cells in response to TLR activation. *The Journal of experimental medicine*, 205(2), 315-322.

87. Vazirinejad, R., Ahmadi, Z., Arababadi, M. K., Hassanshahi, G., & Kennedy, D.

(2014). The biological functions, structure and sources of CXCL10 and its outstanding



part in the pathophysiology of multiple sclerosis. *Neuroimmunomodulation*, 21(6), 322-330.

88. Drappier, M., & Michiels, T. (2015). Inhibition of the OAS/RNase L pathway by viruses. *Current opinion in virology*, 15, 19-26.

89. Yamashita, M., Chattopadhyay, S., Fensterl, V., Saikia, P., Wetzel, J. L., & Sen, G. C. (2012). Epidermal growth factor receptor is essential for Toll-like receptor 3 signaling. *Science signaling*, 5(233), ra50-ra50.

90. De, S., Zhou, H., DeSantis, D., Croniger, C. M., Li, X., & Stark, G. R. (2015). Erlotinib protects against LPS-induced endotoxicity because TLR4 needs EGFR to signal. *Proceedings of the National Academy of Sciences*, 112(31), 9680-9685.]

91. Velepparambil, M., Poddar, D., Abdulkhalek, S., Kessler, P. M., Yamashita, M., Chattopadhyay, S., & Sen, G. C. (2018). Constitutively Bound EGFR–Mediated Tyrosine Phosphorylation of TLR9 Is Required for Its Ability To Signal. *The Journal of Immunology*, 200(8), 2809-2818.

92. Wakatsuki, S., Furuno, A., Ohshima, M., & Araki, T. (2015). Oxidative stress–dependent phosphorylation activates ZNRF1 to induce neuronal/axonal degeneration. *Journal of Cell Biology*, 211(4), 881-896.

93. Hayashi, K., Taura, M., & Iwasaki, A. (2018). The interaction between IKK α and LC3 promotes type I interferon production through the TLR9-containing

LAPosome. *Sci. Signal.*, 11(528), ean4144.

94. Li, Z., Jiang, Y., Jiao, P., Wang, A., Zhao, F., Tian, G., ... & Chen, H. (2006). The NS1 gene contributes to the virulence of H5N1 avian influenza viruses. *Journal of*

virology, 80(22), 11115-11123.

95. Seo, S. H., Hoffmann, E., & Webster, R. G. (2002). Lethal H5N1 influenza viruses escape host anti-viral cytokine responses. *Nature medicine*, 8(9), 950-954.

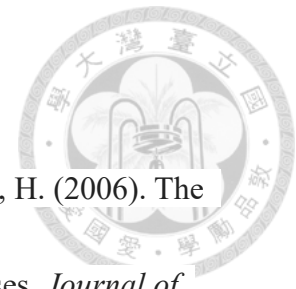
96. Hayman, A., Comely, S., Lackenby, A., Murphy, S., McCauley, J., Goodbourn, S., & Barclay, W. (2006). Variation in the ability of human influenza A viruses to induce and inhibit the IFN- β pathway. *Virology*, 347(1), 52-64.

97. Szretter, K. J., Gangappa, S., Belser, J. A., Zeng, H., Chen, H., Matsuoka, Y., ... & Katz, J. M. (2009). Early control of H5N1 influenza virus replication by the type I interferon response in mice. *Journal of virology*, 83(11), 5825-5834.

98. Salomon, R., Staeheli, P., Kochs, G., Yen, H. L., Franks, J., Rehg, J. E., ... & Hoffmann, E. (2007). Mx1 gene protects mice against the highly lethal human H5N1 influenza virus. *Cell Cycle*, 6(19), 2417-2421.

99. Koutsakos, M., Kedzierska, K., & Subbarao, K. (2019). Immune responses to avian influenza viruses. *The Journal of Immunology*, 202(2), 382-391.

100. Salomon, R., Hoffmann, E., & Webster, R. G. (2007). Inhibition of the cytokine response does not protect against lethal H5N1 influenza infection. *Proceedings of the*



National Academy of Sciences, 104(30), 12479-12481.

101. Almawi, W. Y., Beyhum, H. N., Rahme, A. A., & Rieder, M. J. (1996). Regulation of cytokine and cytokine receptor expression by glucocorticoids. *Journal of Leukocyte Biology*, 60(5), 563-572.

102. Teng, O., Chen, S. T., Hsu, T. L., Sia, S. F., Cole, S., Valkenburg, S. A., ... & Peiris, J. S. M. (2017). CLEC5A-mediated enhancement of the inflammatory response in myeloid cells contributes to influenza virus pathogenicity in vivo. *Journal of virology*, 91(1).

